NILU OR 72/87

NILU OR : 72/87
REFERENCE: N-8434
O-8437
DATE : DECEMBER 1987
ISBN : 82-7247-870-6

THE ABATEMENT OF PHOTOCHEMICAL OXIDANTS IN EUROPE. CALCULATIONS IN SUPPORT OF OECD'S PROJECT "CONTROL OF MAJOR AIR POLLUTANTS"

Øystein Hov

SUMMARY

Model calculations of the long-range transport of photochemical oxidants to 14 rural sites in Europe (one in Austria, three in FRG, two in The Netherlands, one in France, four in Scandinavia and three in the UK) have been carried out for the time period 1 June - 7 June 1982. A lagrangian long-range transport model with the CBM-X chemistry has been applied on the EMEP-grid. The calculations have been compared with hourly measured ozone concentrations, and fair agreement found for the Scandinavian sites and some of the sites in the UK, FRG and The Netherlands.

To be comparable with the NOx-emissions estimated for the PHOXA area for the last days of May 1982, the annual average daily emissions estimated for the EMEP grid cells falling inside the PHOXA area, had to be increased by 40%. The annual average daily VOC emissions for EMEP were comparable to the values estimated in PHOXA. With the assumption that the annual average daily emissions estimated for all of the EMEP grid for 1982 was adjusted upwards by 40%, it is shown that a reduction of the NOx-emissions uniformly over the grid by 25% or more leads to an increase in calculated O_3 at all sites, while a reduction in VOC-emissions by 25% or more is calculated to reduce ozone. A combined reduction or increase in both NOx and VOC emissions by 25%, has little influence on ozone at the 14 receptor sites.

If the NOx-emissions were reduced to the EMEP emissions estimated for that part of 1982 (70% of the annual average), it was found that both NOx- and VOC-emission control, separately or together, efficiently reduced ozone; VOC-emission control being somewhat more efficient than NOx-emission control.

CONTENTS

THE ABATEMENT OF PHOTOCHEMICAL OXIDANTS IN EUROPE. CALCULATIONS IN SUPPORT OF OECD'S PROJECT "CONTROL OF MAJOR AIR POLLUTANTS".

1 INTRODUCTION

Development of emission reduction scenarios of nitrogen oxides (NOx) and volatile organic compounds (VOC) to reduce the formation of photochemical oxidants in Europe, is a part of OECD's project "Control of major air pollutants" (MAP). Combined chemistry and transport models are used to investigate how changing emissions might influence the formation of photochemical oxidants in Europe. It has been decided to concentrate the attention on one period where measurements showed that the concentration of ozone was elevated at many rural sites in several OECD-countries in Europe: 2-5 June 1982.

1.1 OUTLINE OF REPORT

Model calculations using the Norwegian lagrangian long-range transport model with CMB-X chemistry (Whitten et al., 1984) for the time period 1 June 1982, 1200 GMT, to 7 June 1982, 1200 GMT, have been carried out for 14 receptor points within the EMEP grid area, see Table 1 for a list of the sites with geographical coordinates (latitude-longitude) and EMEP-coordinates, see Figure 1 for a map of the EMEP grid. Calculations have been carried out every 6 h GMT, i.e. at arrival times 0000, 0600, 1200 and 1800 GMT at each site.

Sensitivity calculations have been carried out for 19 different emission reductions of NOx and VOC.

In the report is given a brief outline of the Norwegian long-range transport model for photochemical oxidants and a description is given of the input data (emissions, meteorology, ground removal).

Following the model description, the results of the calculations are discussed, starting with the model validation where calculated and

measured ozone concentrations for the 14 receptor points are discussed. Afterwards the results of the sensitivity calculations are discussed.

Table 1: Receptor points in the model calculation

Site No.	Site	Country	Latitude ^{0}N	Longitude (^{0}E > 0, ^{0}W < 0)	EMEP-coordinates x	y
1	Illmitz	A	47.77	16.77	26.01	16.83
2	Langenbrügge	FRG	52.80	10.75	21.10	17.42
3	Schauinsland	FRG	47.92	7.90	22.55	13.61
4	Deuselbach	FRG	49.77	7.05	21.88	14.46
5	Risø	DK	55.00	11.00	20.04	18.73
6	Rørvik	S	57.42	11.93	19.07	20.32
7	Langesund	N	59.00	9.75	17.63	20.60
8	Jeløy	N	59.40	10.75	17.72	21.08
9	Sappermeer	NL	53.10	6.47	19.45	16.30
10	Waarde	NL	51.25	4.05	19.40	14.47
11	Colomiers	F	43.37	1.20	21.70	8.42
12	Bottesford	UK	52.56	-0.48	17.04	14.11
13	Sibton	UK	52.50	1.50	17.85	14.57
14	Stodday	UK	54.10	3.20	17.80	16.02

2 MODEL DESCRIPTION

2.1 PREVIOUS APPLICATIONS

The Norwegian lagrangian long-range transport model with atmospheric boundary layer chemistry was described by Eliassen at al. (1982a).

In the first application of the model, ozone formation and transport to southern Norway and south-eastern Sweden during the time period 6-14 April 1979 was studied (Eliassen et al., 1982a). The air flow was primarily over eastern Europe towards southern Scandinavia.

In the second application of the model, the formation of oxidants during transport to southern Scandinavia during the time period 26 August to 14 September 1980 was studied (19 days). Ozone and PAN measurements at a number of sites in Scandinavia were used in the model validation. The flow direction was predominantly from the south-west and south during the time period (Hov et al., 1985).

A third application was reported by Hov (1987) for the time period 28 May-3 June 1982 with calculations of the formation of photochemical transport along trajectories to the same sites as listed in Table 1.

2.2 METEOROLOGICAL MODEL

The model has been described in some detail previously (Eliassen et al., 1982a, Eliassen et al., 1982b, Hov et al., 1984). The pollutants are assumed to be completely vertically mixed throughout the boundary layer which has a variable depth along the 96 h long 850 mb trajectories. No mass transport takes place through the top of the well-mixed layer. Lateral diffusion is not treated explicitly, but the emission data are given in a 150 km grid where finer details than 150 km in the concentration fields are smoothed out.

In episode studies with short sampling times (like one hour), the rate of horizontal spread of instantaneous releases of pollutants may be an important parameter which should be considered (Eliassen, 1984). For a sampling time of many hours, like 6 h or more, the instantaneous diffusion of pollutant releases is dominated by the diffusion due to sampling time ("synoptic swinging of the trajectories", Smith, 1979). A sampling time of 24 h is used for sulphur species in EMEP, in which case the synoptic swinging of trajectories is the dominating factor for plume spread (Eliassen, 1984).

During transport, pollutants are emitted into the air parcel according to the emission maps for NOx and VOC. Instantaneous concentrations are predicted upon arrival of a trajectory. The horizontal resolution of the concentration fields is determined by the choice of emission grid and density of trajectory arrival points. The combined effects of vertical wind shear and diffusion due to heat exchange is difficult to handle in lagrangian models. Trajectory models are simple numerically, however, since the integration is reduced to an ordinary time-integration along certain selected trajectories.

Trajectory positions are calculated every 2 h, as described in Petterssen (1956), based on wind observations at the 850 mb level at 0000, 0600, 1200 and 1800 GMT. The observed wind data are analysed

objectively in the EMEP grid, cpr. Figure 1. In regions where wind observations are scarce, such as over sea, the wind analysis is heavily influenced by the quasi-geostrophic balanced wind predicted by the Norwegian Meteorological Institute as part of its weather prediction routine.

Alternative trajectories for transport at the 925 mb level rather than 850 mb, can be calculated by backing the analysed 850 mb wind by e.g. 10^0 and reducing it to 90% or so. Radiosonde observations close to the trajectory can give an indication as to the turning and change in speed of the wind with height. The mixing height used represents a material surface below which both old and new pollutants are mixed. The 1200 GMT mixing height is chosen. The basic data for the mixing height analysis are taken from radiosonde data (about 120 radiosonde reports are available within the grid). The estimated mixing heights are objectively analysed to produce grid values at 1200 GMT every day. At intermediate times it is assumed that each trajectory conserves its mixing height.

Objective analysis of temperature, relative humidity and absolute humidity are carried out at 0000 and 1200 GMT in the 150 km grid, as vertical averages between the surface and the 850 mb level. The temperature is used to evaluate temperature-dependent reaction rate coefficients. The relative humidity is used as a rough indication of cloud cover, which influences the photodissociation rates (see Table 2).

Table 2: Parameterization of cloud cover using the relative humidity.

Relative humidity	Cloud cover	"Effective" albedo
> 85%	1.0	0.6
75-85%	0.5	0.3
< 75%	0.0	0.0

When the relative humidity exceeds 90%, precipitation is assumed, and a wet deposition rate coefficient of $1 \times 10^{-4} s^{-1}$ is applied to the concentrations of H_2SO_4, HNO_3, H_2O_2 and CH_3O_2H. For lower relative humidities than 90%, a first order wet deposition rate coefficient of

$5 \times 10^{-6} s^{-1}$ is applied. The individual trajectories are assigned mean values of temperature and absolute humidity at 0000 and 1200 GMT. The temperature is estimated by linear interpolation and the absolute humidity is conserved at intermediate positions.

2.3 DRY DEPOSITION

Dry deposition velocities appropriate for 1 m height are given in Table 3.

Table 3: Dry deposition velocities appropriate for 1 m above the ground.

Component	Deposition velocity (cm/s)	Comments
O_3	0.5	daytime over land surfaces
O_3	0.05	nighttime over land
O_3	0.0	sea surfaces
NO_2	0.5	daytime over land
HNO_3	1.0	determined by aerodynamic resistance

To arrive at a model where average boundary layer concentrations are calculated rather than the concentration at 1 m, the deposition velocities given in Table 3 for O_3, NO_2 and PAN were simply reduced by 50%. Detailed calculations for June 1985 using meteorological data from the Numerical Weather Prediction Model at The Norwegian Meteorological Institute for surface pressure, surface stress, sensible heat flux density and temperature at 2 m height together with data for the surface roughness length and Businger's equations which relate the deposition velocity at the top of the surface layer (50 m height) to the deposition velocity at 1 m above the ground, show that the deposition velocity for SO_2 at 50 m typically was 50-75% of the

value at 1 m (Hov et al., 1987). A reduction by a factor of 2 therefore means that the efficiency of the ground removal processes in the model perhaps are underestimated.

2.4 PHOTOCHEMICAL MODEL

The carbon bond mechanism denoted CBM-X was used in the model. It is described in detail by Whitten et al. (1984). This scheme describes the formation and decompositon of 63 chemical species through 146 chemical reactions. There are 10 classes of hydrocarbons (UNR, ETH, OLE, PAR, TOL, XYL, FORM, ALD2, KET and ACET). The photolysis rate coefficients for NO_2, $O_3 \longrightarrow O(^1D)$, HCHO, ALD2 (= CH_3CHO) are calculated explicitly through the integration over the absorption spectrum of the product of the wavelength dependent quantum yield, the absorption cross section and the solar flux at a given time and location. The photolysis rate coefficients of the other species which are photolysed, are calculated as a fixed fraction of the photolysis rate coefficient for NO_2. The CBM-X mechanism is documented in Appendix 1.

An updated version of the surrogate mechanism used in the calculations with the Norwegian long-range transport model (Eliassen et al., 1982a; Hov et al., 1984) was also used for comparison with the results using the CBM-X mechanism. Of the hydrocarbon emissions, 30% by volume (on a compound basis) are represented as C_2H_6, 20% as nC_4H_{10}, 20% as C_2H_4, 10% as C_3H_6 and 20% as m-xylene. The chemical scheme and the representation of the hydrocarbon emissions are discussed in more detail by Eliassen et al. (1982a) and Hov et al. (1984). It consists of about 100 chemical reactions including photochemical reactions, and 40 different species.

Dissociation rate coefficients are calculated for every 5^0 latitude and every 15 min of the day. The total vertically integrated atmospheric ozone column is adjusted to correspond to the season and latitude. Points along a given trajectory are allocated dissociation rate coefficients through interpolation in time and space to the appropriate latitude and local time.

In the RTM III-model calculations, a condensed version of CBM-X is used (CBM-IV). CBM-IV, has 70 chemical reactions, 24 chemical species (excluding SO_2 and sulphate), and 9 hydrocarbon classes. It is described by Whitten and Gery (1985). CBM-IV has only fairly recently become available for use within the PHOXA-project outside of the RTM III-model. A comparison of the results of 5 days of calculations in a continental photochemical box model using the surrogate mechanism in the Norwegian long-range transport model, CBM-X and other chemical schemes, was reported by Hov et al. (1986). It turned out that the CBM-X chemistry gave somewhat lower ozone concentrations than the surrogate mechanism, a result which is confirmed in the present report.

2.5 INITIAL CONDITIONS

The initial concentrations assigned at the starting point of the 96 h long trajectories can be important for the development along the trajectory. Ground removal is the ultimate removal mechanism for ozone, and in cases with low deposition, the lifetime of ozone is much longer than four days.

In such situations four days' trajectories may not be sufficient to trace the history of an air mass. If the weather is fair at the starting point, the air masses arriving there may have accumulated photochemically active pollution for a number of days.

The integration is started with a set of concentrations corresponding to a slightly polluted atmosphere, with the removal proceses in equilibrium with NOx and NMHC emissions at 10% of the average emissions for Western Europe. The initial concentrations of the most important species are listed in Table 4.

Table 4: Initial concentrations (ppbv).

Specie	Concentration	Specie	Concentration
NO	0.001	O_3	32
NO_2	0.3	HNO_3	1.0
NMHC (C)	2.2	PAN	0.04

2.6 EMISSIONS

Much work is being done to improve European emission inventories for SO_2, NOx, VOC and also NH_3. Within the PHOXA-project, annual and episode specific emissions for SO_2, NOx, CO and 10 hydrocarbon classes according to the requirement of CBM-X, have been established. The PHOXA-grid and the extension to be used in the RTM III-calculation for OECD are shown in Figure 2. Episode specific emissions with hourly values of NO, NO_2, SO_2, CO and 10 hydrocarbon classes for 31 May and 1-2 June 1982 for the PHOXA-grid, were made available to NILU by TNO.

It is apparent from Figure 2 that it is not straightforward to transfer PHOXA-grid emissions to the EMEP-grid. This not only applies to the EMEP grid squares fully outside of the PHOXA-grid, but also to the EMEP-grid squares only partially covered by PHOXA-grid elements.

For the EMEP-grid, unofficial inventories of NOx and VOC-emissions exist, starting with an inventory which was thought to be representative for about 1980 (Eliassen et al., 1982a). As information from the EMEP-countries on national NOx-emissions is coming in to EMEP MSC-W at The Norwegian Meteorological Institute and to EMEP CCC (at NILU), improved and updated NOx-inventories for the EMEP-grid are established.

During the last 1-2 years activity has been organized also through OECD to collect emission data for the OECD countries in Europe in a grid which coincides with the EMEP-grid, but with grid elements of size 50 x 50 km^2 rather than 150 x 150 km^2 at 60^0N latitude. The collection of emission data within OECD and PHOXA has improved the data availability in western Europe, but the very important assessment of emissions in East Europe and the western part of USSR, has to be done through EMEP.

For the part of the PHOXA-grid which fully covers EMEP-grid squares (i.e. excluding the parts of the PHOXA-grid which only partially cover EMEP grid cells), the contents of the PHOXA episode specific emission data file for 31 May - 2 June 1982, are summarized in Table 5.

Table 5: Total emissions in the PHOXA episode specific emission file for the grid cells which fully covers EMEP grid cells, translated into annual figures.

Date	NOx (kt(NO_2)/y)	VOC (kt/y)
31 May 1982	14326	9580
1 June 1982	14173	10783
2 June 1982	14170	11747

For the emission inventory published by Eliassen et al. (1982a), valid for about 1980, the corresponding figures to Table 5 for NOx-emissions was 10113 kt(NO_2)/y and 10793 kt/y for VOC. It can be seen that the average VOC-emissions were similar, while the PHOXA-specific NOx-emissions were about 40% higher than the estimate for the EMEP-grid. However, the VOC-emissions for the PHOXA-grid contain a very significant fraction (about 2/3) thought to be natural hydrocarbons (terpenes and isoprene) for this episode where the temperatures were high over large parts of Europe. The VOC-emissions estimated for the EMEP-grid were anthropogenic only, as an annual average. In CBM-X, natural VOC's are treated as a mixture of paraffinic and olefinic bond type molecules.

To arrive at an emission inventory for the EMEP-grid for June 1982, it was decided to keep the grid distribution for NOx and VOC as estimated for 1980, but increasing the NOx-values for all of the EMEP grid by 40% to get agreement with the PHOXA-area estimate. Furthermore, the average distribution on hydrocarbon classes as found from the PHOXA episode specific emission file, was applied, see Table 6. The original split into hydrocarbons in the surrogate mechanism was retained, however (see section 2.4).

In this way some of the main features from the PHOXA episode specific emission file are retained in the calculation reported here.

Table 6: Distribution of VOC-emissions on hydrocarbon classes, on a mass basis.

Hydrocarbon class	Percent of total VOC emission on a mass basis
OLE	11
PAR	66
TOL	3
XYL	4
FORM	1
ALD2	7
KET	1
ACET	1
ETH	2
UNR	4
CO	350

2.7 MATHEMATICAL FORMULATION

The mass conservation equation determining the concentration c_i of species i can be written as

$$\frac{Dc_i}{dt} = -(\frac{v_d}{h} + k_w)\, c_i + \frac{E_i}{h} + S_i$$

The notation is

D/dt	Lagrangian (total) time derivative along a trajectory
$v_d(x,y,t)$	dry deposition
$h(x,y,t)$	mixing height
$k_w(x,y,t)$	wet deposition rate
$E_i(x,y)$	direct emission of pollutant
S_i	chemical sources or sinks.

In the integration procedure the appropriate back trajectories are first calculated from the analysed wind fields. Then the quantities v_d, h, k_w, etc. originally given as Eulerian fields, are converted into lagrangian information, i.e. as a function of transport time

along the trajectories. These operations transform the mass conservation equation into an ordinary differential equation in time. Lastly, this equation is integrated to obtain calculated instantaneous concentrations at the receptor points.

The integration of the mass conservation equation is done with a quasi-steady-state approximation method (QSSA). This metod is explicit and applies a fixed time step. The upper limit for the computational error is estimated to be 5%.

3 MODEL CALCULATIONS 1 JUNE - 7 JUNE 1982

3.1 EPISODE DESCRIPTION

There was a high pressure system located over north Europe with its center over Denmark on 30 May 1982, moving eastward and with its center over East Europe on 2 June. Winds were weak and predominantly from the southeast, with clear skies. A number of thunderstorms were recorded during the 1 June - 7 June 1982 period. Temperatures in the north European continent ranged between 16^0 - 20^0C, in Scandinavia $20\text{-}25^0$C. The maximum observed ozone concentration was 165 ppb.

In Figures 3a-g is shown the 96 h, 860 mb, back trajectories at 1200 GMT to the 14 receptor points described in Table 1, for each of the days 1 June - 7 June 1982. For 1 - 5 June the winds were low, the transport direction variable and the transport distance over 96 h fairly modest. On the 6 and 7 June the Norwegian sites were influenced by air from the northwest, while the sites in the UK and the southern part of the Netherlands and FRG got air transported from the southeast.

The mixing height field for 1200 GMT each day 1 - 7 June 1982 is shown in Figures 4a-g. The field is calculated by an objective analysis of the mixing height as measured by about 120 radiosondes within the grid. In particular over oceans the results is quite much influenced by the initial guess (1000 m) and in areas with very few soundings, one sounding heavily influences the mixing height field over several grid lengths in all directions. When looking at Figures 4a-4g together

with the map in Figure 1, it can be seen that in general the mixing height has a maximum over continental Europe and the Soviet Union exceeding 1500-2000 m. Over the Atlantic and in the Mediterranean the mixing height in general is lower than over the continents, perhaps by as much as 500-1000 m. There are many exceptions and in some cases one or a few radiosonde observations with high mixing heights give rise to values over 2000 m also over oceanic and coastal areas.

In Figure 5a an example is given of the relative humidity field. The values are low over continental Europe in the high pressure system, and higher over oceanic regions. The relative humidity in this case is derived from the radiosonde data, where temperature and dew point temperature at constant pressure surface and at significant levels, are recorded. From these data relative humidity is derived and gridded values obtained through objective analysis. In Figure 5b, an example of the temperature field is shown (in ^{0}C).

3.2 CALCULATIONS AND MEASUREMENTS

Hourly measurements of ozone were available for 13 of the 14 sites in Table 1 for the period 1 - 7 June 1982. The measurements are taken very near the ground surface, usually only one or a few metres above the ground. This means that the measured concentrations usually are significantly reduced at night through ground removal below the nocturnal inversion and by local emissions of NOx becoming trapped in the shallow nocturnal mixed layer. On the other hand, in the model a concentration representative of a layer with height comparable to the noon mixing height the day before, is calculated at night. This concentration is only weakly influenced by ground removal at night, and therefore the calculated diurnal variation of O_3 is usually smaller than the measured. It should be kept in mind that for measured and calculated ozone concentrations, only the day time values when the atmospheric boundary layer is well mixed, are really comparable.

In Figures 6a-6n the measured and calculated O_3-concentrations for the 14 sites are shown. In the case of Langenbrügge, measurements of ozone were not available.

In Figure 6a is shown the results for Illmitz, which is located in a rural area in eastern Austria at 117 m.a.s.l. Illmitz has a record of measuring high ozone concentrations, as can be seen for April-September 1985 in Table 7 where ozone measurements from 24 European rural sites are presented (Grennfelt et al., 1987). It can be seen that at Illmitz, more than half of the hourly values exceeded 60 ppb, while at the station with the second highest number of measurements exceeding 60 ppb, Schauinsland, about 1/4 of the values exceeded 60 ppb. Schauinsland is a high elevation site 1205 m.a.s.l, and is more representative of the atmosphere above the boundary layer. The difference between Illmitz and all the other sites is perhaps even more striking for the measurements where very high ozone concentrations were found. In 1985 46 hourly values exceeded 140 ppb at Illmitz, the only other site measuring above 140 ppb was Langenbrügge, and only once. The highest value measured at Illmitz in 1985 was 223 ppb, almost twice as high as the station with the second highest ozone maximum (Jeløya in Norway; 133 ppb).

In Figure 6b-6d the results for the sites in FRG are shown. The measurements at Schauinsland reflect that it is a high altitude site with only a slight diurnal variation, indicating that the air which is brought over the station has not recently been near the ground or polluted with NOx-emissions. The calculated values are lower than the measured values in the first part of the period (1-4 June).

Deuselbach is located 480 m.a.s.l. on rural land which is partly cultivated and partly pasture. The calculations fit quite well.

The measurements and calculations at the four Scandinavian sites Risø, Rørvik, Langesund and Jeløya are shown in Figures 6e-6h. All these sites are coastal or near coastal. The calculations are less satisfactory for Risö and Rörvik than for the two Norwegian sites. When measured values are fairly low, e.g. 40-50 ppb, and the calculations do not match, it is likely that the initial concentrations for the calculation may not be well chosen and have a strong influence on the calculated receptor point concentrations.

Table 7: Number of hours (h) and days (d) with hourly ozone concentrations exceeding 120, 160, 200, 240 and 280 $\mu g/m^3$, and maximum hourly and daily ozone concentration ($\mu g/m^3$), April-September 1985. Concentrations in ppb are obtained by division with 2 (Grennfelt et al., 1987).

	Number of hours and days												Maximum ozone concentrations	
	Total		>120		>160		>200		>240		>280		($\mu g/m^3$)	
STATION	h	d	h	d	h	d	h	d	h	d	h	d	h	d
Illmitz	4044	172	2226	168	994	123	405	65	152	32	46	13	446	197
Gent St. Kruiswinkel	3695	161	77	15	38	7	17	4	1	1			253	120
Risø	2875	122	107	22	19	4	3	1					210	146
Brotjacklriegel	3609	152	314	41	8	3							174	109
Deuselbach	4003	170	264	38	31	6							196	109
Langenbrügge-Waldhof	4198	183	473	67	149	23	76	15	15	7	1	1	286	138
Schauinsland	4281	183	1170	91	99	20	4	2					202	127
Westerland	4329	183	101	19	4	2							166	105
Utö	1415	58	26	7	1	1							198	120
Eibergen	3841	165	81	17	18	7							181	99
Witteveen	2582	87	88	16	17	6	3	1					217	112
Birkenes	1401	61											115	70
Jeløya	4306	181	53	12	22	5	14	5	1	1			266	118
Langesund	2648	110	29	5									133	113
Aspvreten	2928	121	272	30	62	6							198	173
Norra Kvill	1830	77	13	2	3	1							194	100
Ringamåla	3300	138	207	28	17	5	1	1					202	130
Rörvik	3954	172	233	39	35	8	5	1					214	127
Vavihill	3447	144	255	32	44	7	2	1					212	141
Vindeln	1808	78											120	65
Bottesford	4375	183	84	12	22	2	9	1					220	133
Harwell	3805	160	121	23	16	4	1	1					206	136
Wray	4223	181	51	11	4	1							176	113
Sibton	2228	99	50	11	5	1							192	125

The results for the Dutch sites Sappermeer and Waarde are shown in Figures 6i-6j. There is some underestimation of the maximum values measured at Sappermeer on 1-4 June, and even much more so in the case of the southern station located in Waarde.

For the French site Colomiers in the Pyrenees, the agreement between measurements and calculations is rather poor for 1 - 3 June (Figure 6k), while for the British sites (Figures 6l-6n) the agreement is good for Bottesford, fair for Sibton and a failure to pick up the high concentrations measured at Stodday on 1 - 2 June.

It should be remembered, however, that the distance between these sites is so small that they are found in the same or neighbouring grid elements. It is not to be expected that the data input to the calculations is sufficiently accurate and resolved in time and space to be able to pick up a peak measured value of about 140 ppb at Stodday and 60-70 ppb at Bottesford and Sibton on 2 June 1982.

To conclude, the agreement between the calculated and measured ozone concentration is fair for the sites in Scandinavia, FRG, UK and the Netherlands, and poor for the French and Austrian sites.

3.3 EMISSION REDUCTIONS AND CHANGES IN O_3, PAN AND NO_2

Calculations have been carried out to see how the concentrations of O_3, PAN and NO_2 at the 14 receptor sites specified in Table 1, change during the 1 - 7 June 1982 period with changes in the emissions of NOx and VOC.

Uniform emission changes were carried out throughout the EMEP grid, and the scenarios are outlined in Table 8. The runs m-s are similar to the runs a-g with the NOx-emissions reduced by a factor 2. This means that the "reference case" for the runs m-s is run d, where NOx is reduced by 50% compared to run 0. Since run 0 corresponds to a run where the NOx-emissions are 1.4 times the EMEP annual average emissions on a daily basis, run d corresponds to a case where the NOx-emissions are 70% of the annual average. This is what normally is assumed for May/June-emissions in the EMEP calculations.

Table 8: Emissions for NOx and VOC in % of the reference.

	Emissions in % of the reference case.	
Run No.	NOx	VOC
0	100	100
a	100	75
b	100	50
c	75	100
d	50	100
e	75	75
f	125	125
g	25	25
h	40	51
i	100	51
j	40	100
k	40	88
l	100	88
m	50	75
n	50	50
o	37.5	100
p	25	100
q	37.5	75
r	62.5	125
s	12.5	25

Runs h-l in Table 8 were set up on the basis of information in the OECD-document ENV/AIR/87.2 (1st revision), dated 20 August 1987 and circulated to the delegates to the Air Management Policy Group. The best available control technology for NOx and VOC leads to reductions in the NOx- and VOC-emissions as shown in Table 9, reproduced from the OECD-document mentioned above. The same document gave information on the total NOx- and VOC-emissions per source category in OECD Europe in 1980, and these numbers are reproduced in Table 10. These total OECD-Europe, anthropogenic NOx- and VOC-emissions per source category, were then uniformly reduced throughout the EMEP-grid based on the reductions specified in Table 9. All of the NOx-emissions were assumed to be anthropogenic, while for VOC two cases were considered: The natural VOC-emissions equal to 20% of the total, which is approximately what is estimated as an annual average for the PHOXA-area, and the natural VOC-emissions equal to 75% of the total VOC-emissions, which is approximately what is estimated for the sun light and temperature conditions which prevailed during the May-June 1982 high pressure situation. Case h in Table 8 is the emissions when 20% of the VOC emissions are natural, and in case k 75% of the VOC-emissions are natural. Case

k should be considered to be the emission reduction scenario most in line with the "best available control technology" for the 2-5 June 1982 time period.

Table 9: Reductions in NOx- and VOC-emissions on the basis of the best available control technology.

Source category	Emission reduction technology	Overall NOx emission reduction (%)
Road Traffic		
Gasoline Cars	3 way catalyst	80
Diesel Cars	engine modifications & EGR	70
Diesel Trucks	" "	70
Power plants		
Major Point Sources	SCR	70
Remainder	low NOx burners	50
Industrial Combustion		
Major Point Sources	SCR	70
Remainder	combustion modifications	25
Source category	**Emission reduction technology**	**Overall VOC emission reduction (%)**
Road Traffic		
Gasoline Cars	3 way catalyst	90
Solvent Use		
Industrial	carbon adsorption	60
Non-Industrial		
- Dry Cleaning	adsorption or condensation	80
- Painting	reformulation of paint	70
Gasoline Petroleum Industry		
Storage/Transfer	internal floating roof tanks with secondary seals, vapour recovery system on transfers	80

Table 10: Anthropogenic NOx and VOC emissions per source category in OECD Europe in 1980 (tonnes) and fraction of total in %.

	NOx (NO_2)	%	VOC	%
Mobile Sources	5608036	53	3954189	48
Road traffic	3917172	37	3040253	37
Other mobile sources	454464	4	186936	2
Power Plants	2577278	24	46030	1
Non-industrial combustion	678821	6	376215	5
Industry	1661315	16	1086955	13
Combustion	1260155	12	41638	1
Process	401160	4	509252	6
Storage and handling	0	0	354665	4
Organic solvent evaporation	0	0	2504612	31
Industrial solvent use	0	0	820470	10
Non-industrial solvent use	0	0	887742	11
Waste treatment and disposal	24030	0	46740	1
Agriculture and food industry	6900	0	187400	2
Miscellaneous	31000	0	0	0
Sum	10587380	100	8202141	100

Table 11: Emission changes (ΔNOx in NOx-emissions, ΔVOC in VOC) and the number of ozone values greater than certain limits (in ppb) for each of the 14 sites for the period 1 - 7 June 1982 (25 arrival times for each site) and added up over all sites (total of 25 x 14 = 350 trajectories). CBM-X chemistry.

REFERENCE RUN, CBM-X chemistry																
Site No.	1	2	3	4	5	6	7	8	9	10	11	12	13	14	Sum	%
> 50	4	20	20	22	17	16	18	17	19	15	2	9	8	6	194	55.4
> 60	1	15	8	18	12	11	11	11	13	6	0	4	3	3	116	33.1
> 70	0	6	3	8	1	3	8	7	8	3	0	3	1	1	52	14.9
> 80	0	2	1	3	0	3	3	3	5	0	0	0	0	0	20	5.7
> 90	0	0	0	0	0	0	1	0	4	0	0	0	0	0	5	1.4
Country	A	FRG	FRG	FRG	DK	S	N	N	NL	NL	F	UK	UK	UK		

(a) ΔNOx 0%, ΔVOC-25%																
Site No.	1	2	3	4	5	6	7	8	9	10	11	12	13	14	Sum	%
> 50	2	16	16	15	12	7	12	14	8	5	1	5	2	2	117	33.4
> 60	0	7	4	4	4	3	8	8	1	1	0	4	0	1	45	12.9
> 70	0	1	0	0	0	2	3	2	1	0	0	0	0	0	9	2.6
> 80	0	0	0	0	0	0	2	0	0	0	0	0	0	0	2	.6
> 90	0	0	0	0	0	0	0	0	0	0	0	0	0	0	0	.0

(b) ΔNOx 0%, ΔVOC-50%																
Site No.	1	2	3	4	5	6	7	8	9	10	11	12	13	14	Sum	%
> 50	0	4	6	2	7	3	6	7	1	0	0	3	0	1	40	11.4
> 60	0	0	0	0	0	0	2	3	0	0	0	0	0	0	5	1.4
> 70	0	0	0	0	0	0	0	0	0	0	0	0	0	0	0	.0
> 80	0	0	0	0	0	0	0	0	0	0	0	0	0	0	0	.0
> 90	0	0	0	0	0	0	0	0	0	0	0	0	0	0	0	.0

(c) ΔNOx - 25%, ΔVOC 0%																
Site No.	1	2	3	4	5	6	7	8	9	10	11	12	13	14	Sum	%
> 50	3	23	21	24	23	20	19	19	23	18	2	9	17	9	230	65.7
> 60	2	18	9	21	18	15	14	11	20	11	0	5	7	5	156	44.6
> 70	1	9	4	12	8	14	10	9	17	4	0	2	1	2	93	26.6
> 80	1	2	1	7	4	6	8	6	10	3	0	0	1	0	49	14.0
> 90	0	0	0	4	1	2	2	0	8	0	0	0	0	0	17	4.9

(d) ΔNOx - 50%, ΔVOC 0%																
Site No.	1	2	3	4	5	6	7	8	9	10	11	12	13	14	Sum	%
> 50	2	22	15	25	23	20	18	19	24	19	0	9	15	9	220	62.9
> 60	2	13	6	22	15	15	14	11	21	10	0	5	8	7	149	42.6
> 70	1	8	3	10	10	12	10	10	16	5	0	1	2	2	90	25.7
> 80	1	3	0	7	6	9	8	7	12	2	0	0	0	0	55	15.7
> 90	0	2	0	4	4	5	5	2	9	0	0	0	0	0	31	8.9

(e) ΔNOx - 25%, ΔVOC - 25%

Site No.	1	2	3	4	5	6	7	8	9	10	11	12	13	14	Sum	%
> 50	2	21	15	22	21	17	18	18	21	12	1	7	9	6	190	54.3
> 60	1	8	4	14	11	12	10	10	13	5	0	4	3	3	98	28.0
> 70	0	2	1	6	2	4	4	4	7	2	0	1	1	0	34	9.7
> 80	0	0	0	2	0	0	1	0	5	0	0	0	0	0	8	2.3
> 90	0	0	0	0	0	0	0	0	4	0	0	0	0	0	4	1.1

(f) ΔNOx + 25%, ΔVOC + 25%

Site No.	1	2	3	4	5	6	7	8	9	10	11	12	13	14	Sum	%
> 50	9	21	22	22	16	15	18	17	18	13	2	10	8	7	198	56.6
> 60	1	16	14	18	11	9	12	12	13	6	1	5	3	2	123	35.1
> 70	0	7	6	11	5	4	8	8	7	4	0	4	0	2	66	18.9
> 80	0	3	2	2	0	3	6	6	5	2	0	2	0	0	31	8.9
> 90	0	1	0	1	0	2	3	3	2	0	0	0	0	0	12	3.4

(g) ΔNOx - 75%, ΔVOC - 75%

Site No.	1	2	3	4	5	6	7	8	9	10	11	12	13	14	Sum	%
> 50	1	3	0	5	6	10	9	4	11	1	0	0	0	0	50	14.3
> 60	0	0	0	1	1	0	0	0	5	0	0	0	0	0	7	2.0
> 70	0	0	0	0	0	0	0	0	2	0	0	0	0	0	2	.6
> 80	0	0	0	0	0	0	0	0	0	0	0	0	0	0	0	.0
> 90	0	0	0	0	0	0	0	0	0	0	0	0	0	0	0	.0

(h) ΔNOx - 60%, ΔVOC - 49%

Site No.	1	2	3	4	5	6	7	8	9	10	11	12	13	14	Sum	%
> 50	2	12	6	21	16	15	14	11	19	9	0	6	7	7	145	41.4
> 60	1	5	1	8	7	11	9	7	13	3	0	0	1	0	66	18.9
> 70	0	0	0	2	3	2	3	1	8	0	0	0	0	0	19	5.4
> 80	0	0	0	0	1	0	0	0	5	0	0	0	0	0	6	1.7
> 90	0	0	0	0	0	0	0	0	3	0	0	0	0	0	3	.9

(i) ΔNOx 0%, ΔVOC - 49%

Site No.	1	2	3	4	5	6	7	8	9	10	11	12	13	14	Sum	%
> 50	0	4	6	2	8	3	6	7	1	0	0	3	0	1	41	11.7
> 60	0	0	0	0	0	0	4	3	0	0	0	0	0	0	7	2.0
> 70	0	0	0	0	0	0	0	0	0	0	0	0	0	0	0	.0
> 80	0	0	0	0	0	0	0	0	0	0	0	0	0	0	0	.0
> 90	0	0	0	0	0	0	0	0	0	0	0	0	0	0	0	.0

(j) ΔNOx - 60%, ΔVOC 0%

Site No.	1	2	3	4	5	6	7	8	9	10	11	12	13	14	Sum	%
> 50	2	22	12	23	21	18	17	18	24	18	0	9	13	8	205	58.6
> 60	2	12	4	16	10	15	13	11	21	9	0	5	5	6	129	36.9
> 70	1	5	2	10	8	12	9	10	15	4	0	0	1	2	79	22.6
> 80	0	2	0	7	6	7	8	4	11	1	0	0	0	0	46	13.1
> 90	0	0	0	2	4	4	3	1	8	0	0	0	0	0	24	6.9

(k) ΔNOx - 60%, ΔVOC - 12% Site No.	1	2	3	4	5	6	7	8	9	10	11	12	13	14	Sum	%
> 50	2	20	12	23	21	16	15	17	23	18	0	8	12	8	195	55.7
> 60	1	11	4	15	10	15	12	10	20	7	0	4	4	6	119	34.0
> 70	1	5	2	10	7	11	9	9	13	3	0	0	1	1	72	20.6
> 80	0	2	0	4	4	6	6	2	9	1	0	0	0	0	34	9.7
> 90	0	0	0	2	3	3	1	0	8	0	0	0	0	0	17	4.9

(l) ΔNOx 0%, ΔVOC - 12% Site No.	1	2	3	4	5	6	7	8	9	10	11	12	13	14	Sum	%
> 50	2	19	19	21	16	13	18	17	16	7	2	8	6	3	167	47.7
> 60	0	9	7	12	10	7	8	9	10	5	0	4	3	2	86	24.6
> 70	0	3	2	2	0	3	6	5	4	1	0	2	0	0	28	8.0
> 80	0	1	0	0	0	2	3	2	1	0	0	0	0	0	9	2.6
> 90	0	0	0	0	0	0	1	0	0	0	0	0	0	0	1	.3

Table 12: Percentage of trajectories with more than 60 ppb O_3 at the arrival point for the sites in each of 4 geographical areas and for the sum of those sites. Time period 1 June 1200 GMT-7 June 1982 1200 GMT (25 trajectories per site). CBM-X chemistry.

Run	Description		FRG sites (2+3+4)	Scandinavian sites (5+6+7+8)	NL sites (9+10)	UK sites (12+13+14)	Sum except 1 and 11
	ΔNOx(%)	ΔVOC(%)					
0	0	0	54.7	45.0	38.0	13.3	38.3
a	0	-25	20.0	23.0	4.0	6.7	15.0
b	0	-50	0.0	5.0	0.0	0.0	1.7
c	-25	0	64.0	58.0	62.0	22.7	51.3
d	-50	0	54.7	55.0	62.0	26.7	49.0
e	-25	-25	34.7	43.0	36.0	13.3	32.3
f	+25	+25	64.0	44.0	38.0	13.3	40.3
g	-75	-75	1.3	1.0	10.0	0.0	2.3
h	-60	-49	18.7	34.0	32.0	1.3	21.7
i	0	-49	0.0	7.0	0.0	0.0	2.3
j	-60	0	42.7	49.0	60.0	21.3	42.3
k	-60	-12	40.0	47.0	54.0	18.7	39.3
l	0	-12	37.3	34.0	30.0	12.0	28.7
m	-50	-25	36.0	47.0	52.0	13.3	36.7
n	-50	-50	14.7	31.0	26.0	2.7	19.0
o	-62.5	0	42.7	48.0	58.0	18.7	44.3
p	-75.0	0	29.3	42.0	48.0	9.3	31.7
q	-62.5	-25	32.0	44.0	50.0	10.7	33.7
r	-37.5	25	72.0	65.0	76.0	32.0	60.3
s	-87.5	-75	1.4	0.0	8.0	0.0	1.7

In Table 11 is shown for each station and added over the stations, the number of trajectories with O_3 exceeding some specified value, for the reference run and for the 13 first scenarios described in Table 8.

In Table 12 is shown the percentage of trajectories with more than 60 ppb of ozone at the arrival point for the sites in each of the geographical areas FRG (sites 2-4), Scandinavia (5-8), The Netherlands (9,10) and UK (12-14) and the sum of these 12 sites.

The following conclusions can be drawn:

- Reduction in VOC-emissions by 25%, gives rise to a significant ozone reduction at all sites, a 50% reduction is calculated to keep all O_3-values below 70 ppb.
- Reduction in NOx-emission by 25% is calculated to increase O_3 at all sites, except Illmitz and Colomiers. At the FRG sites, the number of trajectories with more than 60 ppb upon arrival increases from 54.7 to 64.0%, the corresponding numbers for the Scandinavian sites are 45.0 to 58.0%, for the Netherlands 38.0% to 62.0% and for the UK 13.3 to 22.7%.
- A reduction in NOx-emissions by 50% is calculated to further increase O_3 at some sites. For the UK sites the percentage of trajectories with O_3 > 60 ppb is 13.3% in the reference case, 22.7% in the ΔNOx = -25% case and 26.7% in the ΔNOx = -50% case.
- A reduction in NOx and VOC emissions by 25% each is calculated to decrease O_3 slightly, and markedly for the FRG-sites (from 54.7 to 34.7% of the trajectories with O_3 > 60 ppb).
- An increase in NOx and VOC emissions by 25% each is calculated to increase the number of O_3-values above 60 ppb from 116 to 123 added over all sites, above 70 ppb from 52 to 66 cases. Otherwise the influence on ozone is fairly slight. In Scandinavia ozone drops slightly.
- Reduction in NOx and VOC emissions by 75% each is calculated to reduce O_3 significantly everywhere.
- Reduction in NOx and VOC by 60 and 49%, respectively, is calculated to reduce ozone significantly, in particular at the sites in continental Europe.

- Reduction in NOx and VOC by 60 and 12%, respectively, which is the most realistic scenario with best available control technology, then the total number of trajectories with O_3 > 50, 60, 70, 80 or 90 ppb increases. There is an improvement at the FRG sites, while at the sites in the Netherlands the fraction of trajectories with O_3 > 60 ppb increases from 38 to 54%. Also in the UK and in Scandinavia the fraction of trajectories with O_3 > 60 ppb increases.

The effect of reducing the NOx-emissions and VOC-emissions separately or together, was also calculated starting with ΔNOx = -50%, ΔVOC = 0 as the reference case (run d). This corresponds to what is assumed as NOx-emissions for May-June 1982 in the EMEP-inventory given that the annual NOx-emissions are comparable in 1980 and 1982. The effect of emission reductions starting from the new reference case, is quite different from runs a-g.

- A separate reduction in VOC- or NOx-emissions is calculated to reduce ozone at all sites.

- A combined reduction in both VOC- and NOx-emissions are more efficient than reducing only one of them by the same percentage.

- Increase in VOC- and NOx-emissions gives rise to an increase in O_3.

In Table 13 it can be seen that the calculated impact of emission changes on the fraction of trajectories with more than 60 ppb of O_3 upon arrival, is much the same also for the trajectories with more than 1 ppb of PAN. For NO_2 the result is different, reducing HC-emissions is calculated to increase NO_2, reducing NOx-emissions reduce NO_2.

3.4 EMEP-CHEMISTRY

Some of the emission-reduction scenarios were also run with the EMEP-chemistry, updated from Eliassen et al. (1982a). A summary of the results for the fraction of the trajectories were O_3 > 60 ppb at the receptor point, is given in Table 14.

Table 13: Summary of the influence of emission changes on the concentration of O_3, PAN and NO_2 at all 14 receptor sites during the period 1 - 7 June 1982 (1200 GMT), cfr. Table 8.

Run	Description		% of total number of trajectories (350)		
	ΔNOx	ΔVOC	O_3 > 60 ppb	PAN > 1 ppb	NO_2 > 12 ppb
0	0	0	33.1	28.0	3.1
a	0	-25	12.9	8.0	7.4
b	0	-50	1.4	0.3	10.6
c	-25	0	44.6	36.6	0.6
d	-50	0	42.6	34.9	0.0
e	-25	-25	28.0	19.4	0.9
f	+25	+25	35.1	35.7	8.3
g	-75	-75	2.0	1.1	0.0
h	-60	-49	18.9	10.6	0.3
i	0	-49	2.0	0.6	10.6
j	-60	0	36.9	31.7	0.0
k	-60	-12	34.0	28.0	0.0
l	0	-12	24.6	18.6	6.0
m	-50	-25	31.7	22.3	0.3
n	-50	-50	16.6	8.9	0.3
o	-62.5	0	35.4	31.1	0.0
p	-75.0	0	27.4	24.0	0.0
q	-62.5	-25	29.1	22.0	0.0
r	-37.5	25	52.3	46.9	0.6
s	-87.5	-75	1.4	1.1	0.0

Tabell 14: Fraction (%) of total number of trajectories where O_3 > 60 ppb for two different chemistries (CBM-X and EMEP).

Run	Description		% of total number of trajectories (350) where O_3 > 60 ppb	
	ΔNOx	ΔVOC	O_3 CBM - X	EMEP
0	0	0	33.1	51.4
a	0	-25	12.9	33.1
b	0	-50	1.4	13.4
c	-25	0	44.6	65.7
d	-50	0	42.6	64.6
e	-25	-25	28.0	50.9
f	+25	+25	35.1	48.6
g	-75	-75	2.0	17.4

In general the EMEP chemistry predicts higher ozone, which is partly due to a more reactive VOC emissions mix in thh EMEP-formulation of the chemistry. The change in O_3 with changing emissions is quite similar for both formulations of the chemistry.

4 ACKNOWLEDGEMENT

This work is partly sponsored by the Royal Norwegian Research Council for Science and Technology (NTNF). The work has been carried out in co-operation with EMEP MSC-W at the Norwegian Meteorological Institute.

5 REFERENCES

Eliassen, A., Ø. Hov, I.S.A. Isaksen, J. Saltbones and F. Stordal (1982a) A Lagrangian long-range transport model with atmospheric boundary layer chemistry. J. Appl. Met., 21, 1645-1661.

Eliassen, A., Ø. Hov, I.S.A. Isaksen, J. Saltbones and F. Stordal (1982b) A Langragian long-range transport model with atmospheric boundary layer chemistry. In: Air pollution by nitrogen oxides, Eds. T. Schneider and L. Grant. Amsterdam, Elsevier. pp. 347-356.

Eliassen, A. (1984) Aspects of Lagrangian air pollution modelling. In: Air pollution modeling and its application, III, Ed. C. De Wispelaere. N.Y., Plenum Publishing Company. pp. 3-21.

Grennfelt, P., J. Saltbones and J. Schjoldager (1987) Oxidant data collection in OECD-Europe 1985-87 (OXIDATE). Lillestrøm (NILU OR 22/87).

Hov, Ø., K.H. Becker, P. Builtjes, R.A. Cox and D. Kley (1986) Evaluation of the photooxidants-precursor relationship in Europe. Bruxelles, CEC. (Air Pollution Research Report 1).

Hov, Ø., A. Eliassen, D. Simpson, T. Iversen and J. Saltbones (1987) NOx-calculations in EMEP. Report in preparation.

Hov, Ø., A. Eliassen, I.S.A. Isaksen, J. Saltbones and F. Stordal (1984) Regional model for oxidants: The Norwegian long-range transport model with atmospheric boundary layer chemistry. In: Proc. of the EPA-OECD internat. conference on long-range transport models for photochemical oxidants and their precursors, Research Triangle Park, NC (EPA-600/9-84-006).

Hov, Ø, F. Stordal and A. Eliassen (1985) Photochemical oxidant control strategies in Europe: A 19 days´ case study using a Lagrangian model with chemistry. Lillestrøm (NILU TR 5/85).

Hov, Ø. (1987) Modelling of photochemical oxidants and precursors in Europe 28 May - 3 June 1982. Lillestrøm (NILU OR 71/87).

Petterssen, S. (1956) Weather analysis and forecasting. 2. ed. N.Y., McGraw Hill.

Smith, F.B. (1979) The character and importance of plume lateral spread affecting the concentration downwind of isolated sources of hazardous airborne material. In: Proc. WMO Symp. Long Range Transport of Pollutants, Sofia, 1-5 October 1979. Geneve (WMO-No. 538), pp. 241-252.

Whitten, G.Z. and M.W. Gery (1985) Development of CBM-X mechanisms for urban and regional AQSMs. SAI draft report to EPA. (SYSAPP-85/162).

Whitten, G.Z., J.P. Killus and R.G. Johnson (1984) Modeling of auto exhaust smog chamber data for EKMA development. SAI draft report to EPA under Contract No. 68-02-3735.

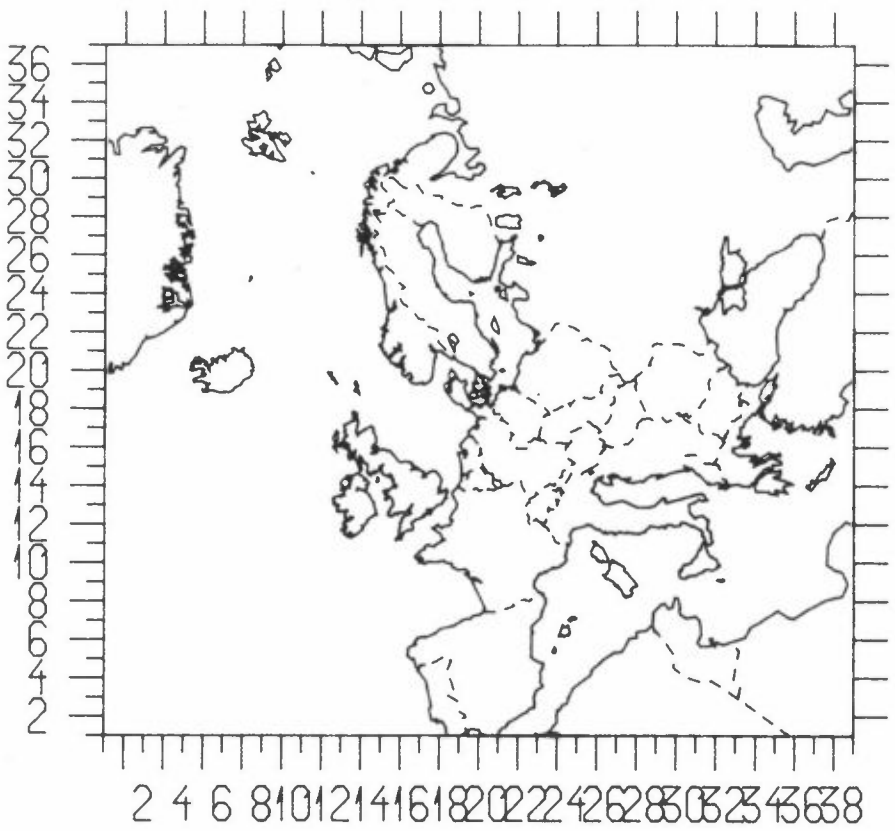

Figure 1: Map of Europe with the grid system used in the EMEP model.

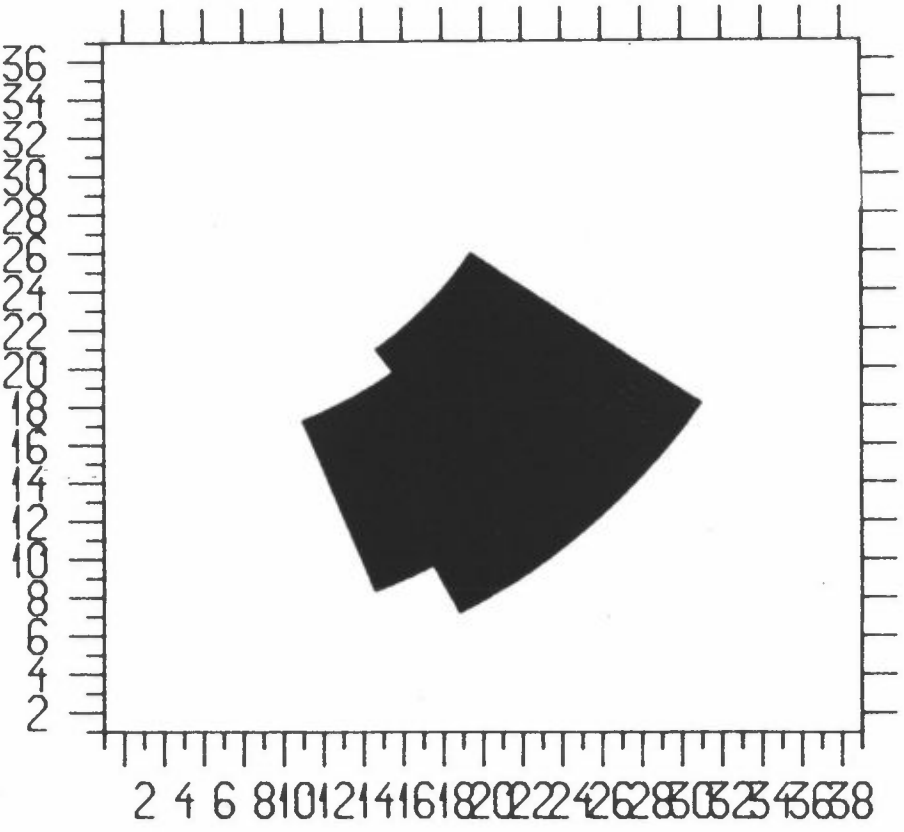

Figure 2: EMEP grid system with the PHOXA (RTM III) grid and the extension of the PHOXA-grid used in calculations for OECD.

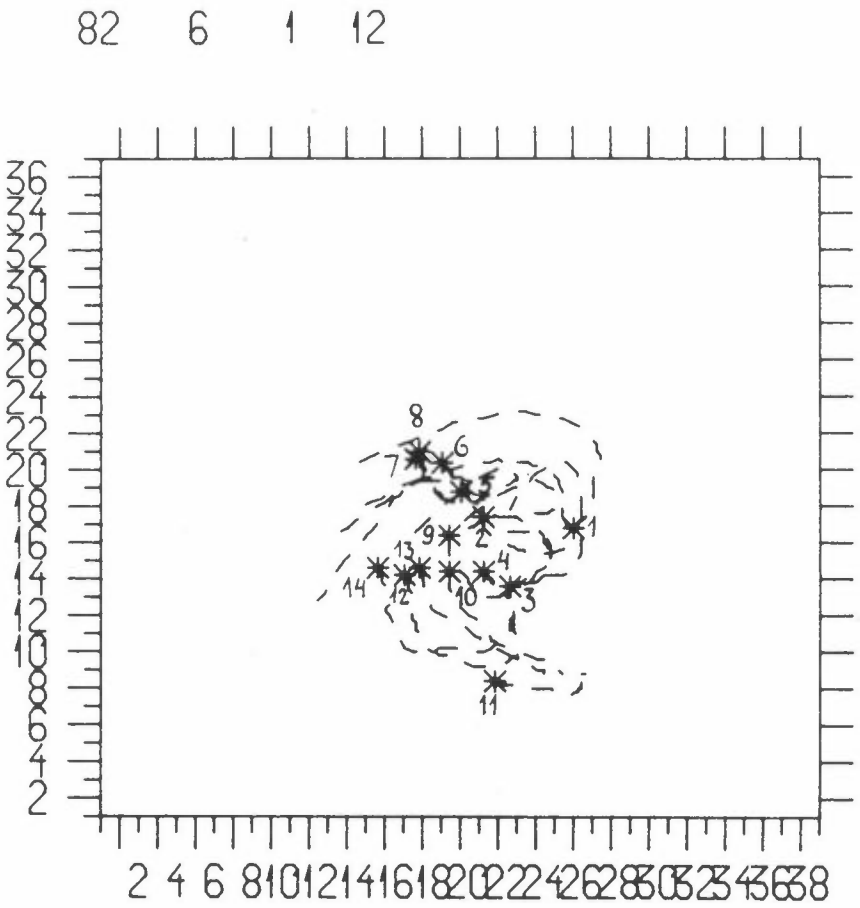
82 6 1 12
8
6
7
9
2
1
13
4
14
12
10
3
11

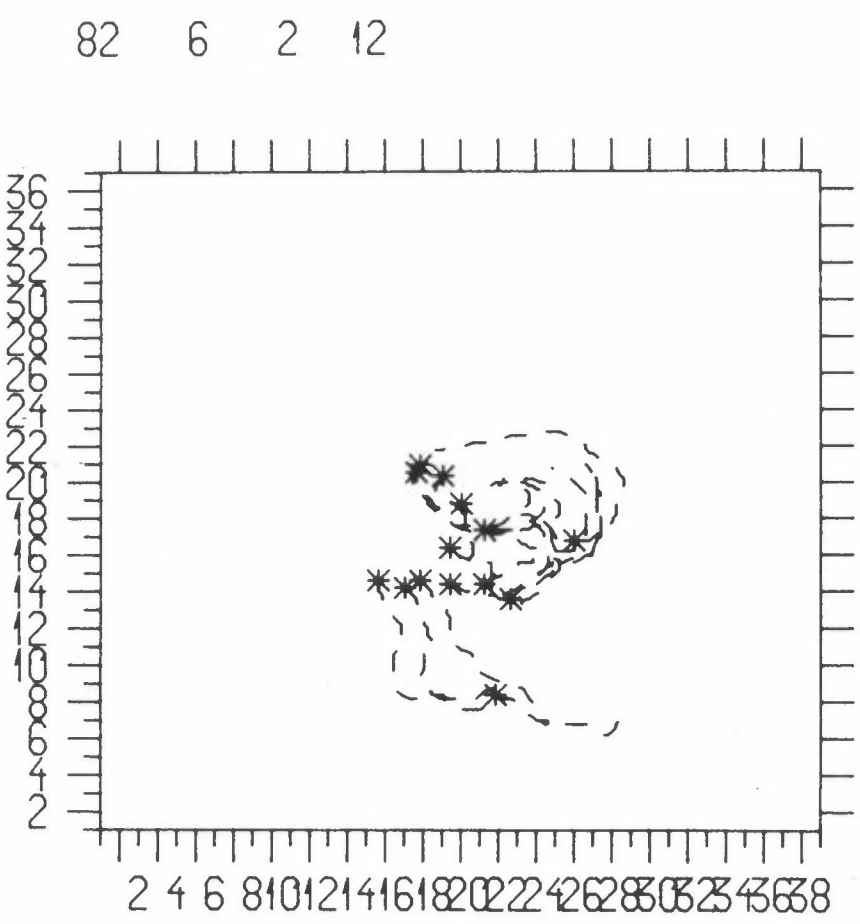
82 6 2 12

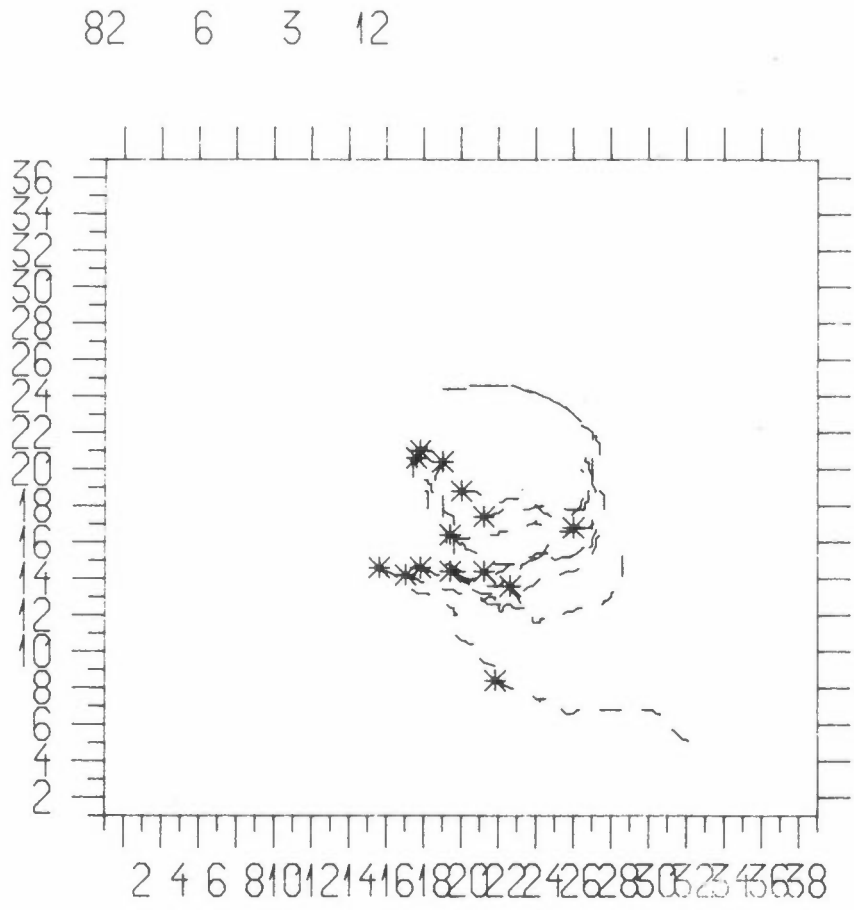
82 6 3 12

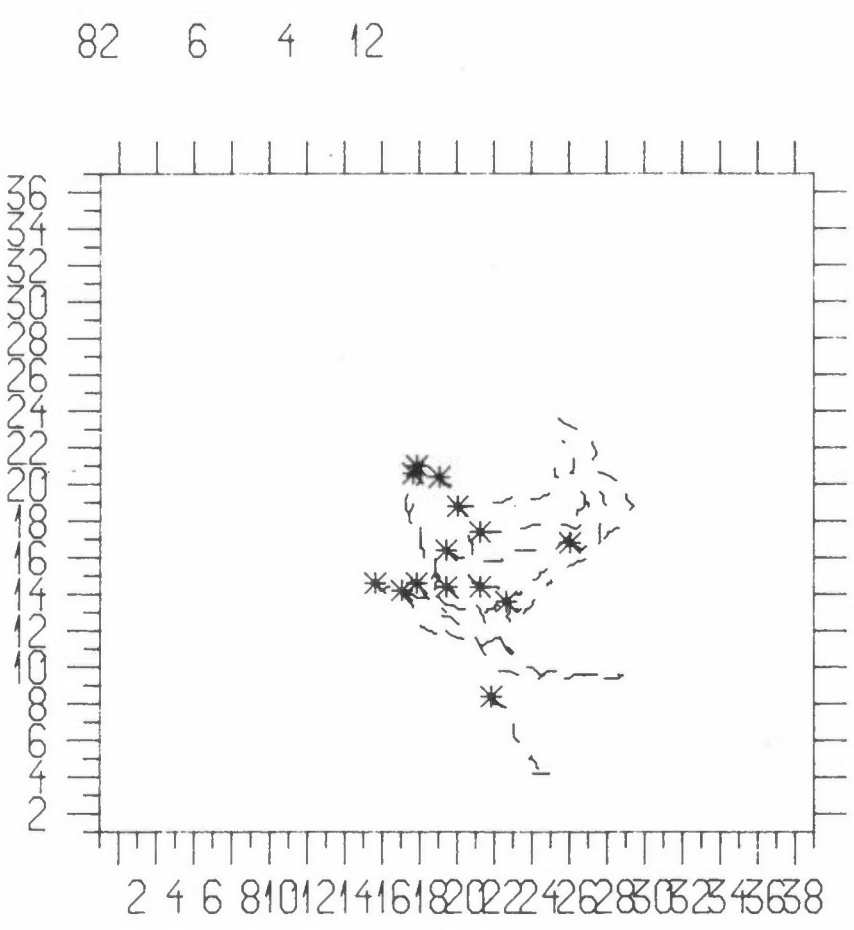
82 6 4 12

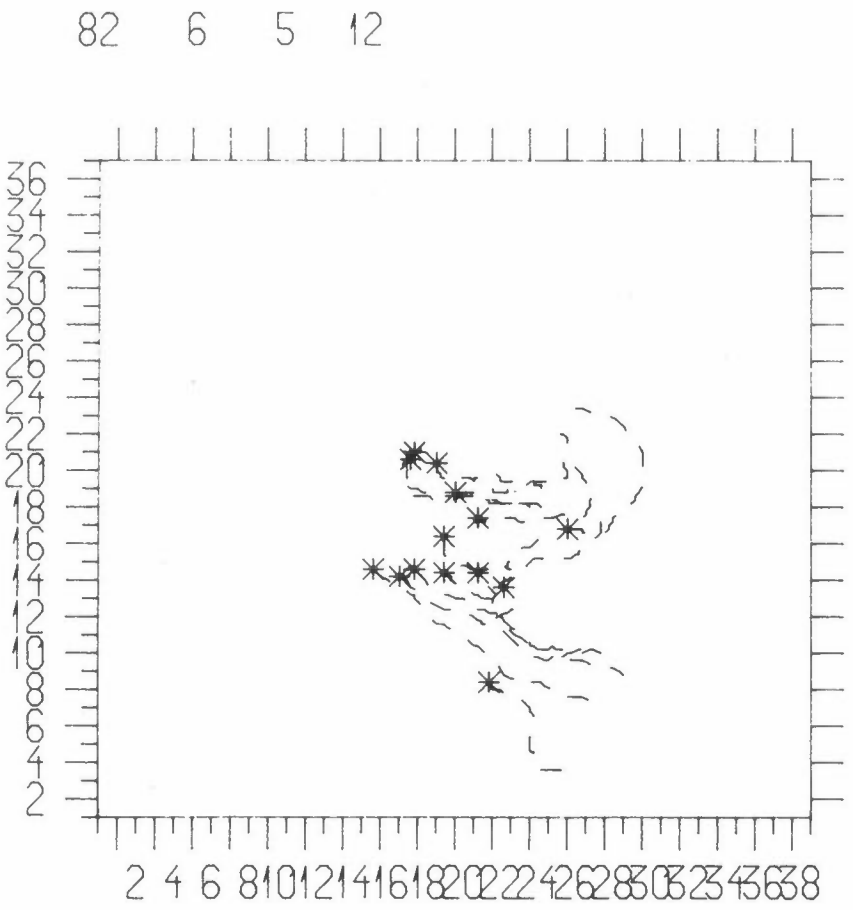
82 6 5 12
36 34 32 30 28 26 24 22 20 18 16 14 12 10 8 6 4 2
2 4 6 8 10 12 14 16 18 20 22 24 26 28 30 32 34 36 38

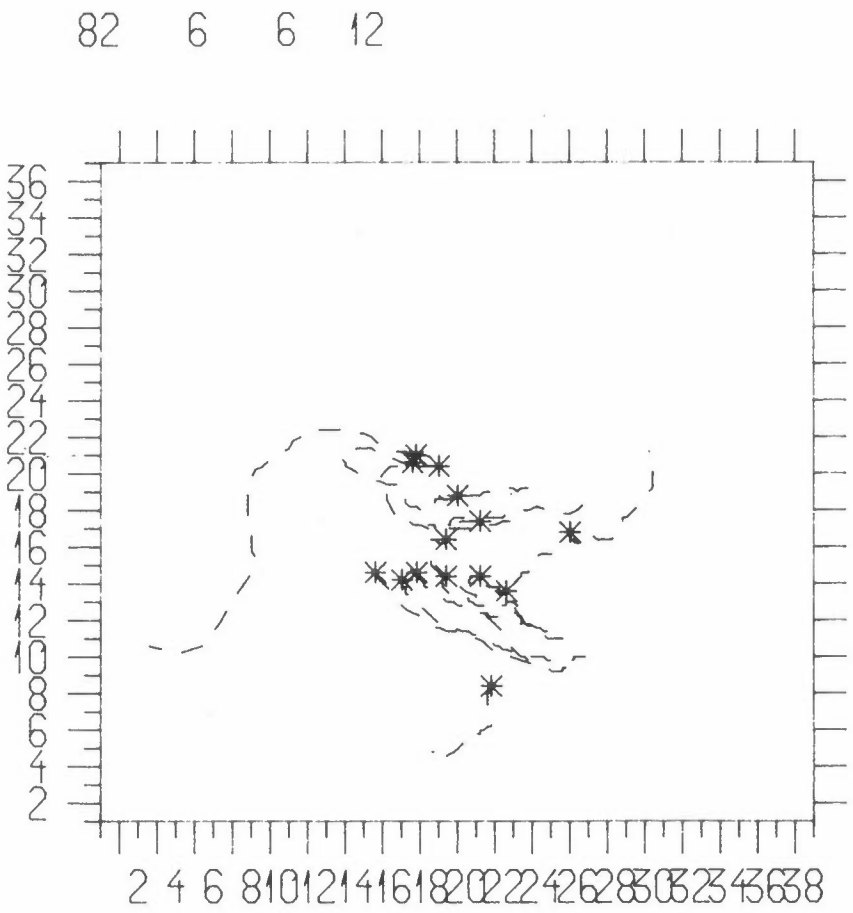
82 6 6 12
36 34 32 30 28 26 24 22 20 18 16 14 12 10 8 6 4 2
2 4 6 8 10 12 14 16 18 20 22 24 26 28 30 32 34 36 38

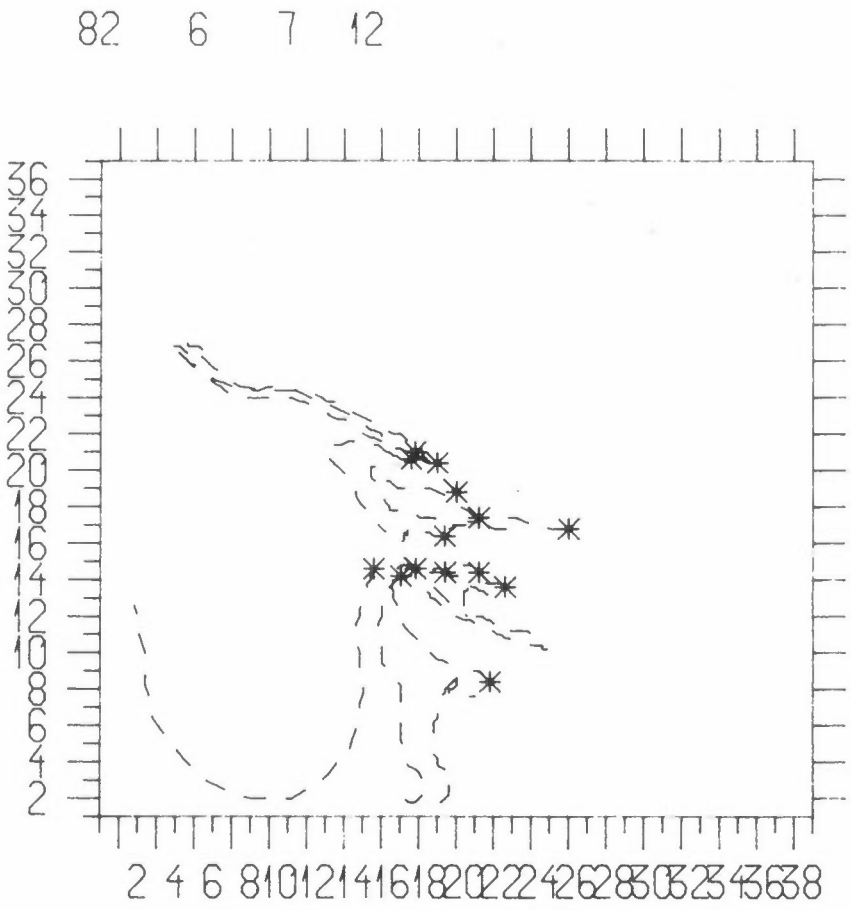

Figure 3: 96 h, 850 mb backtrajectories to 14 sites (Illmitz (1), Langenbrügge (2), Schauinsland (3), Deuselbach (4), Risø (5), Rørvik (6), Langesund (7), Jeløy (8), Sappermeer (9), Waarde (10), Colomiers (11), Bottesford (12), Sibton (13), Stodday (14)) for 1200 GMT each of the days 1 - 7 June 1982.

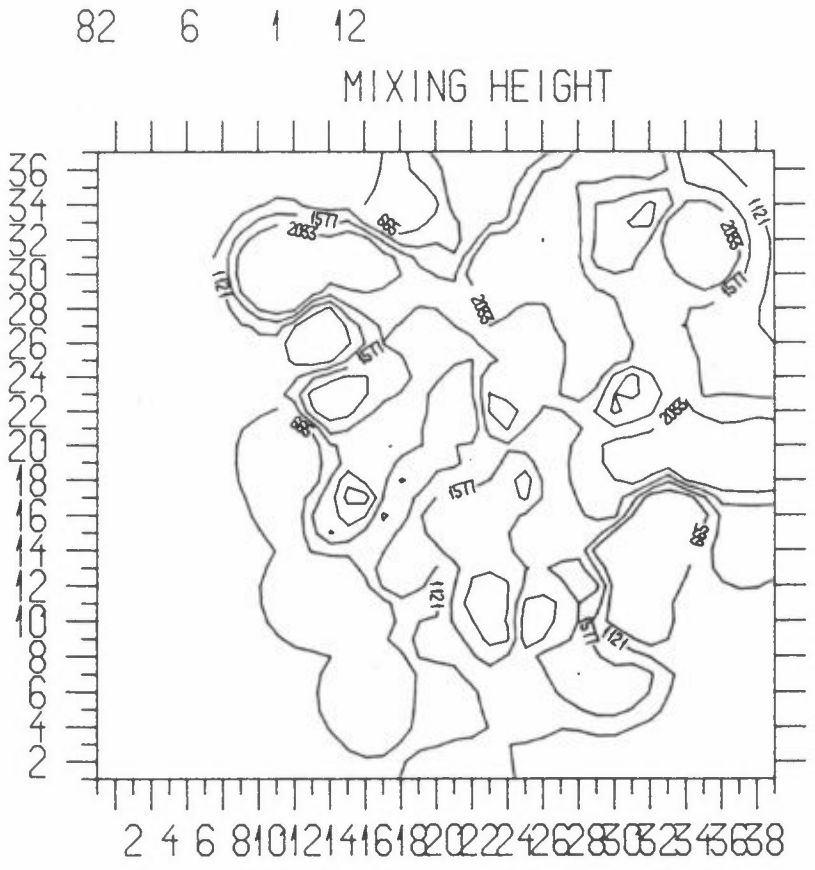

CONTOURS FROM 209. TO 2489., INTERVAL 456.

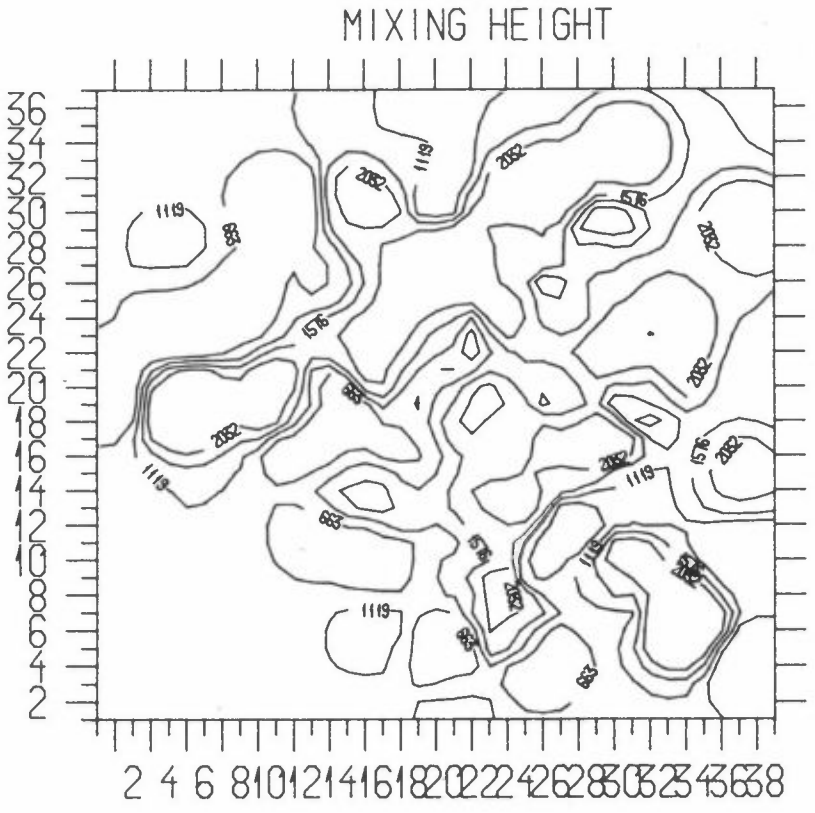

CONTOURS FROM 207. TO 2489., INTERVAL 456.

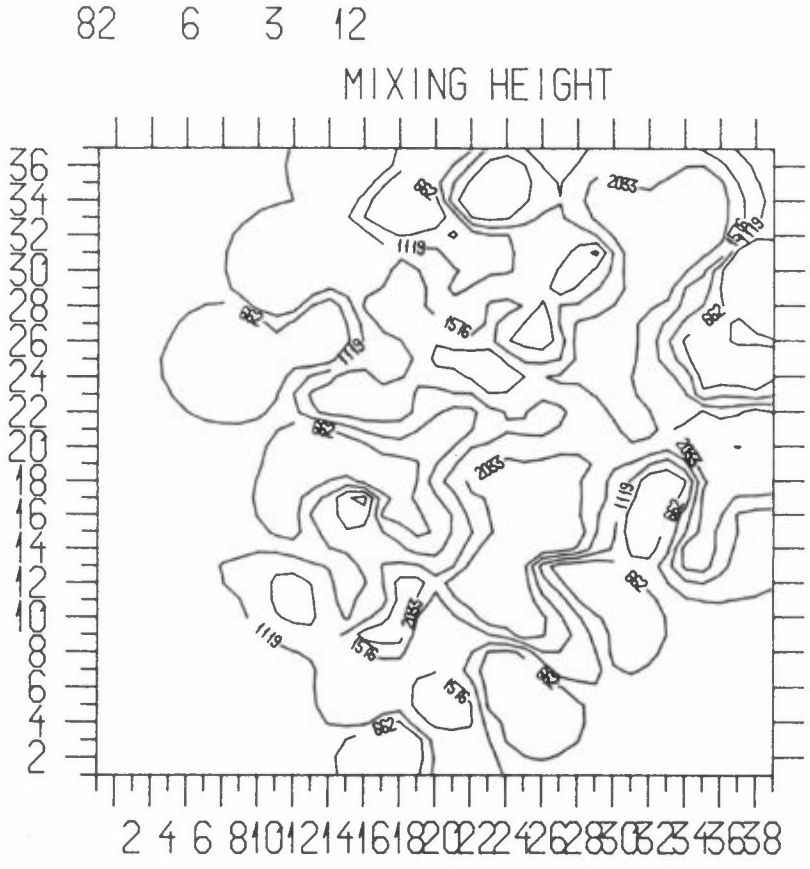

CONTOURS FROM 205. TO 2490., INTERVAL 457.

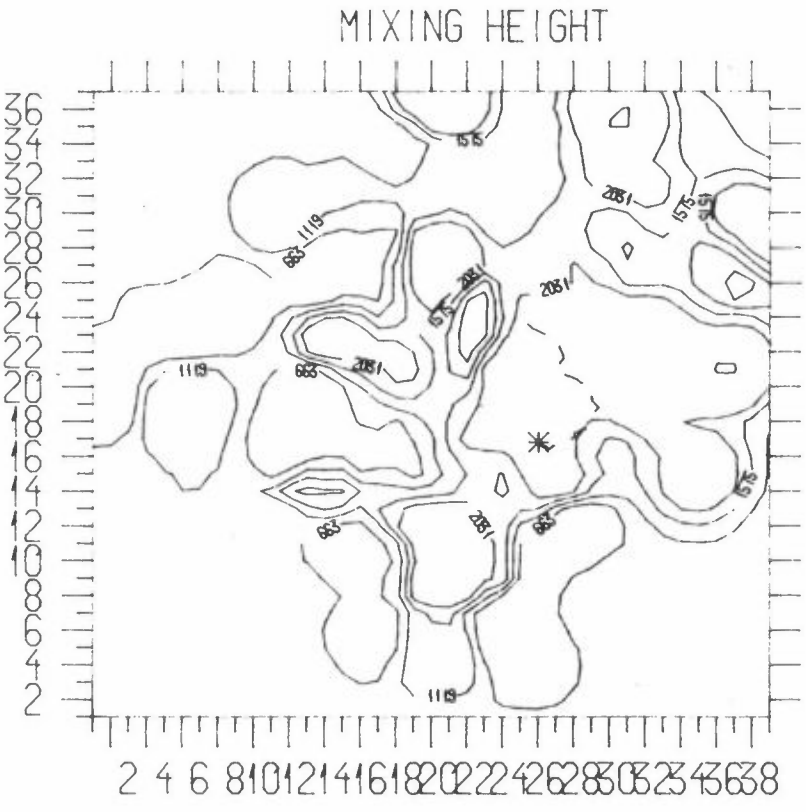

CONTOURS FROM 207. TO 2487., INTERVAL 456.

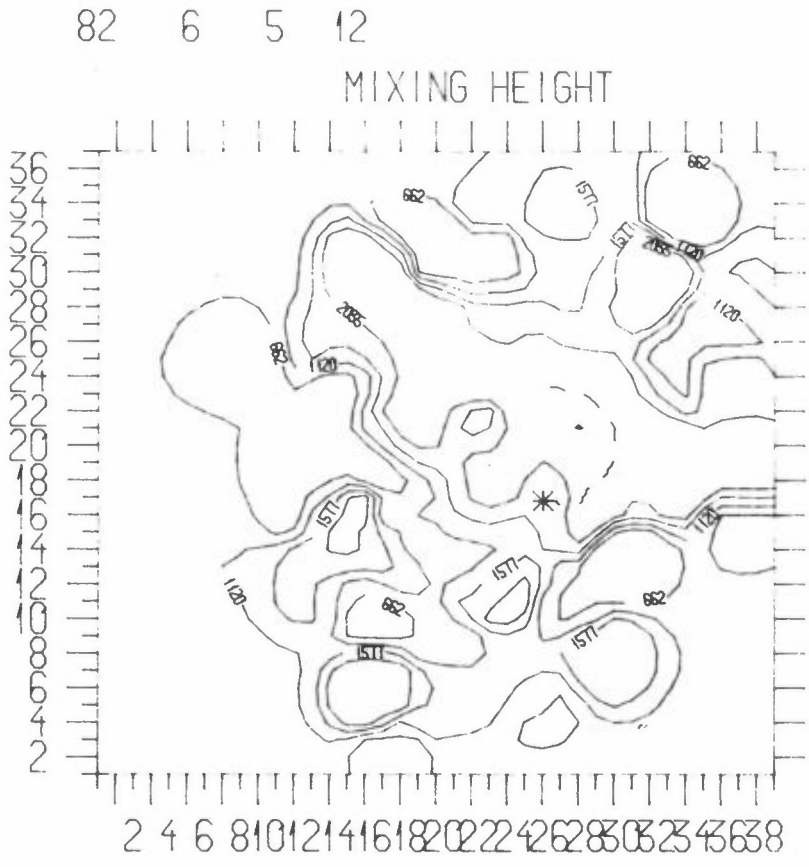

CONTOURS FROM 205. TO 2493., INTERVAL 458.

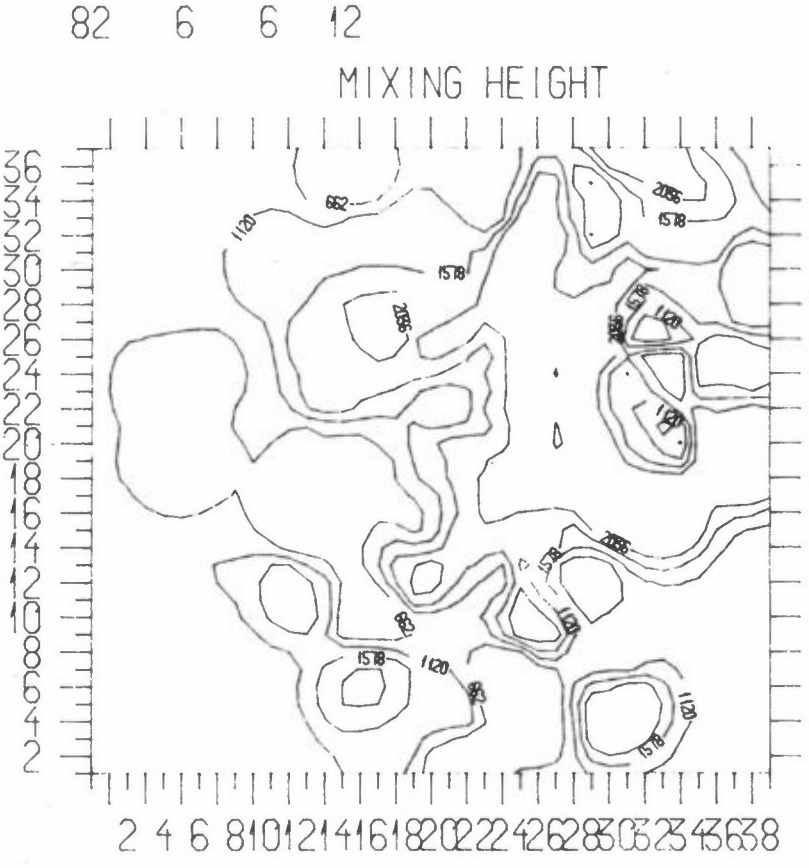

CONTOURS FROM 205. TO 2494., INTERVAL 458.

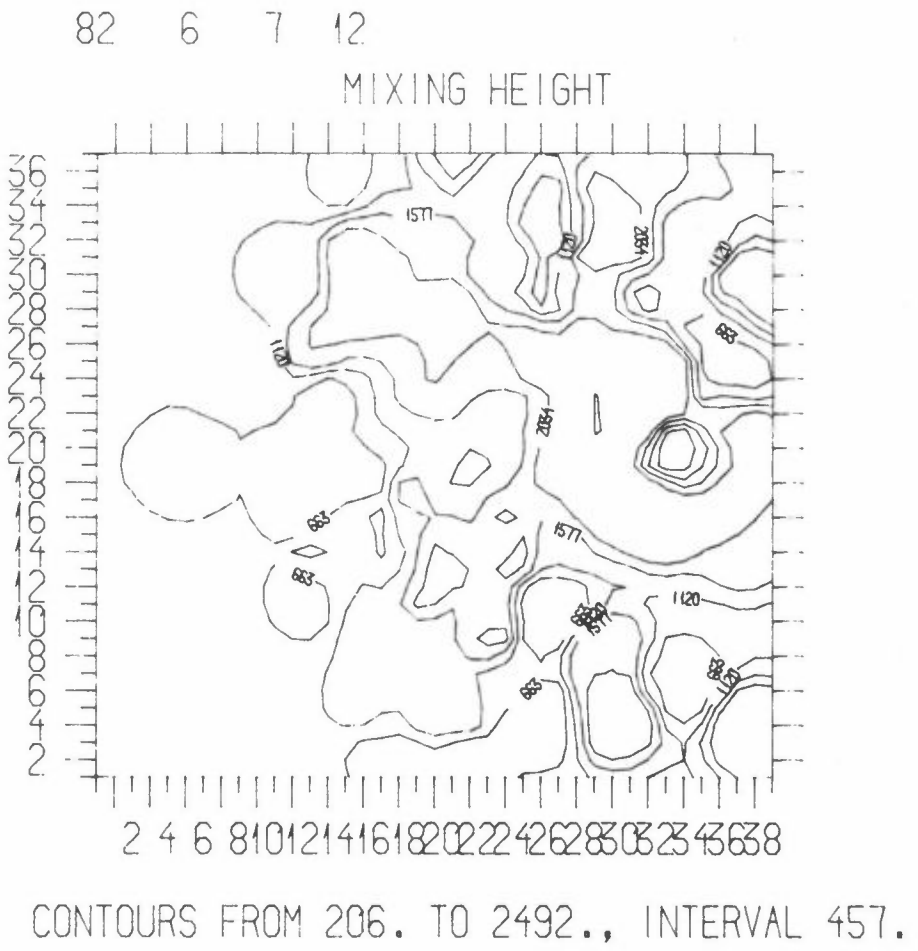

Figure 4: Contours of constant mixing height in m at 1200 GMT each of the days 1 - 7 June 1982.

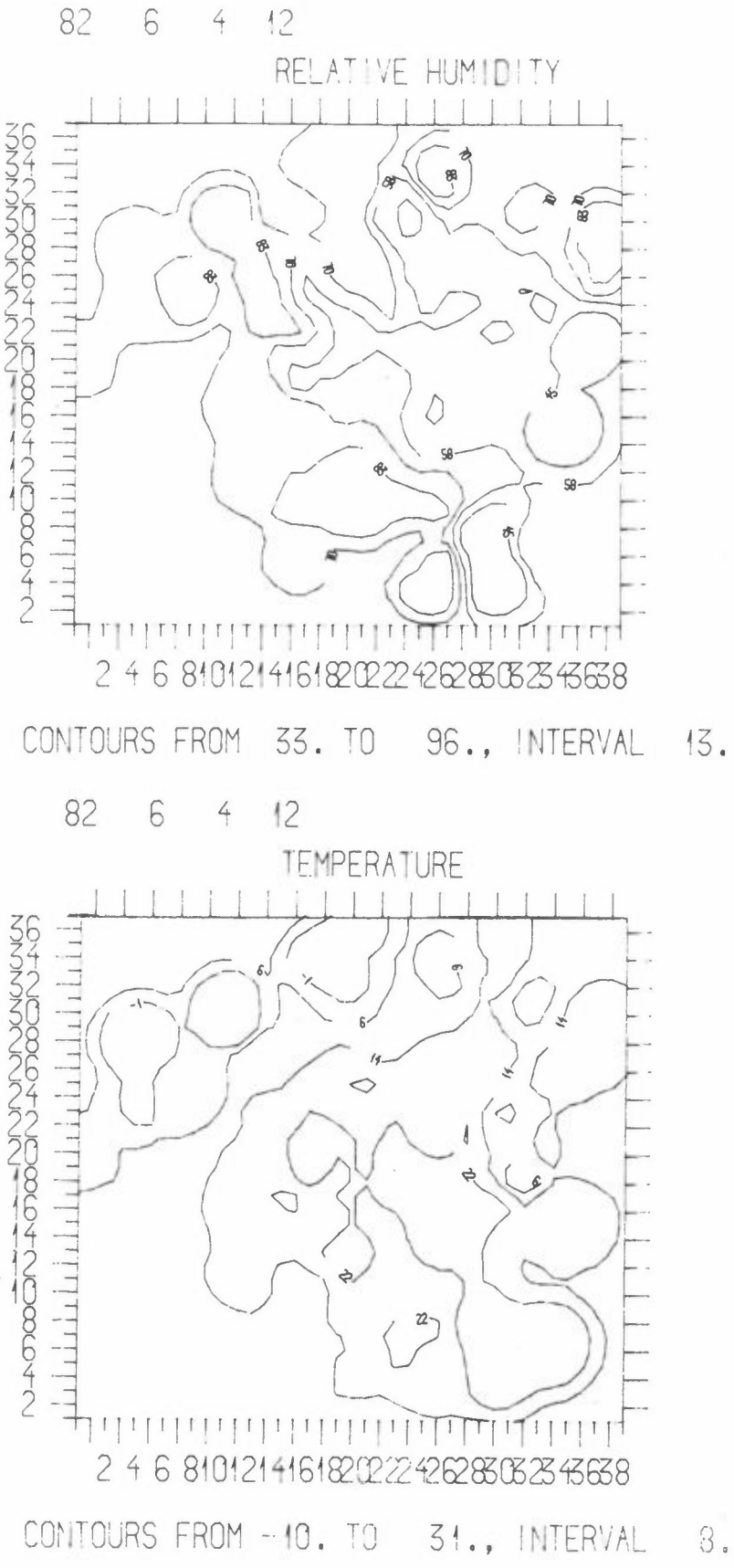

Figure 5: Contours of constant relative humidity (in %) and temperature (in ^{0}C) at 1200 GMT, 4 June 1982.

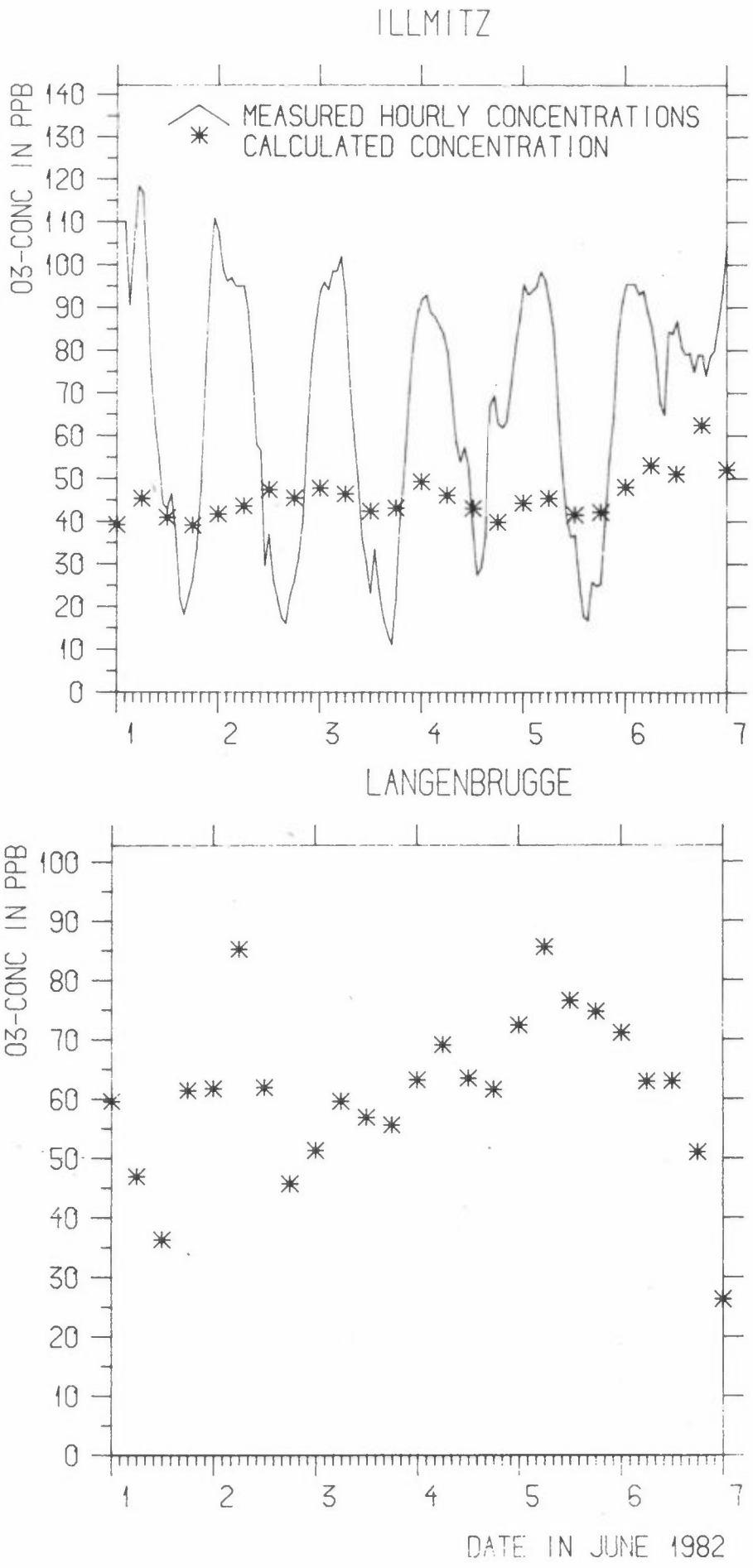
ILLMITZ
MEASURED HOURLY CONCENTRATIONS
CALCULATED CONCENTRATION
O3-CONC IN PPB
0
10
20
30
40
50
60
70
80
90
100
110
120
130
140
1
2
3
4
5
6
7
LANGENBRUGGE
O3-CONC IN PPB
0
10
20
30
40
50
60
70
80
90
100
1
2
3
4
5
6
7
DATE IN JUNE 1982

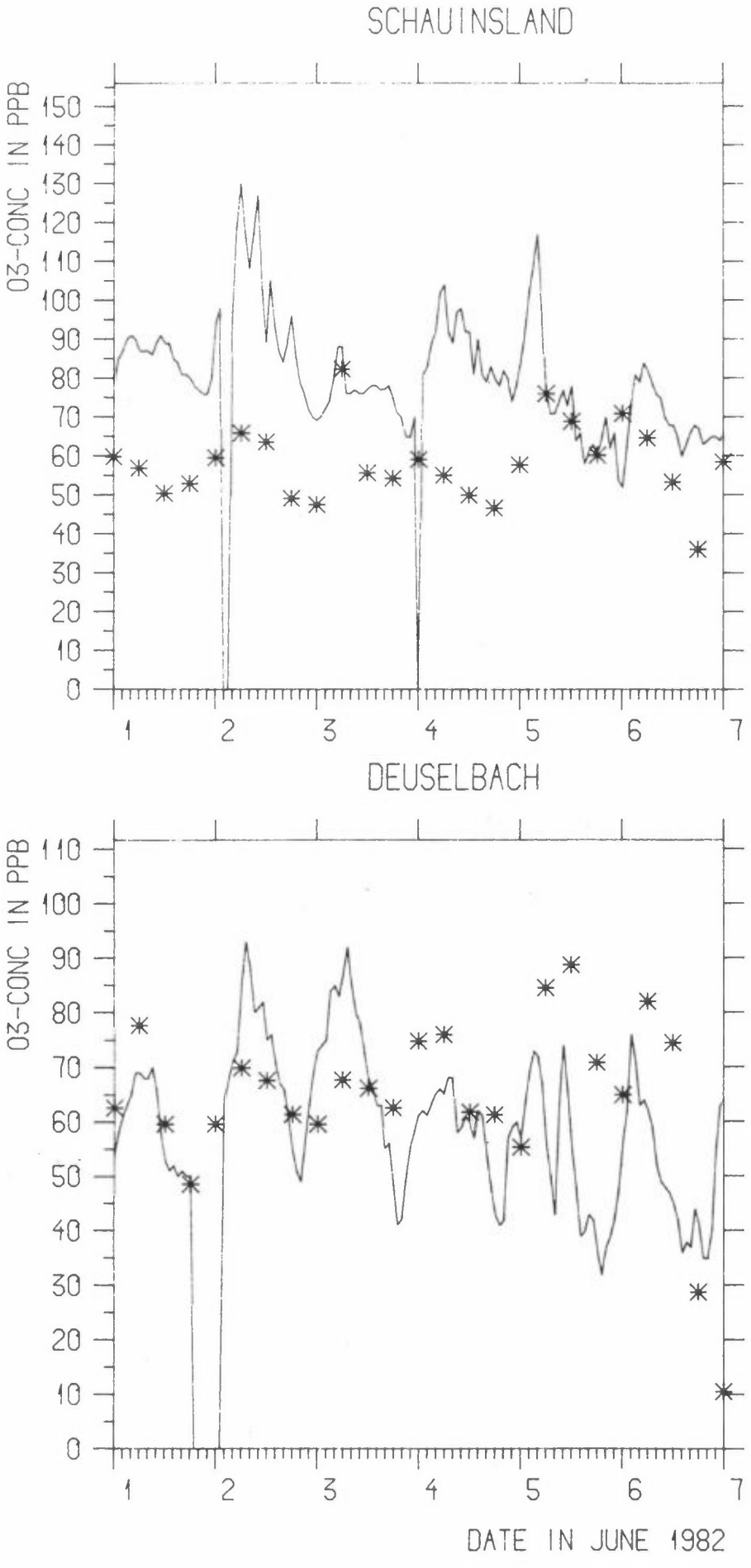
SCHAUINSLAND
O3-CONC IN PPB
150
140
130
120
110
100
90
80
70
60
50
40
30
20
10
0
1
2
3
4
5
6
7
DEUSELBACH
O3-CONC IN PPB
110
100
90
80
70
60
50
40
30
20
10
0
1
2
3
4
5
6
7
DATE IN JUNE 1982

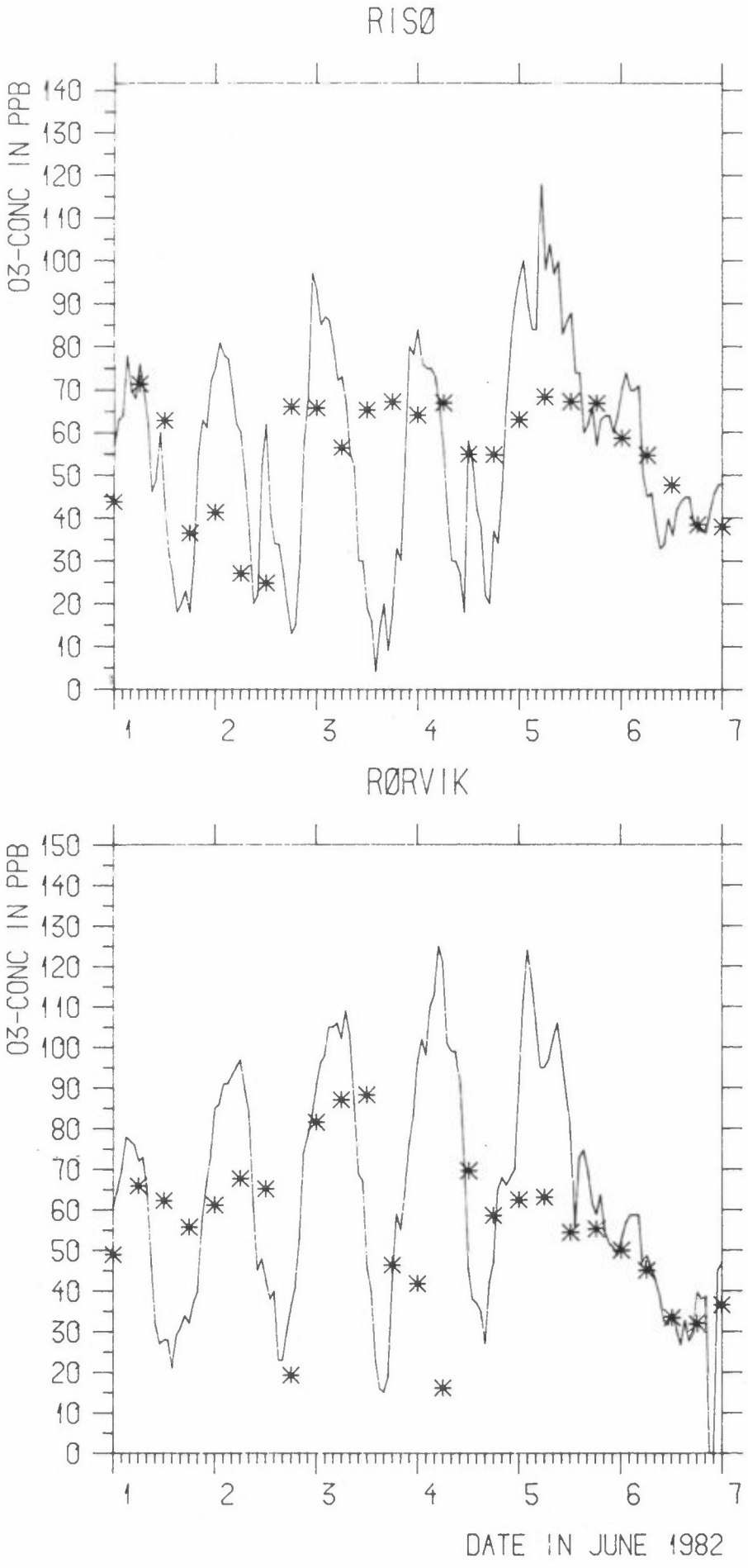
RISØ
O3-CONC IN PPB
0
10
20
30
40
50
60
70
80
90
100
110
120
130
140
1
2
3
4
5
6
7
RØRVIK
O3-CONC IN PPB
0
10
20
30
40
50
60
70
80
90
100
110
120
130
140
150
1
2
3
4
5
6
7
DATE IN JUNE 1982

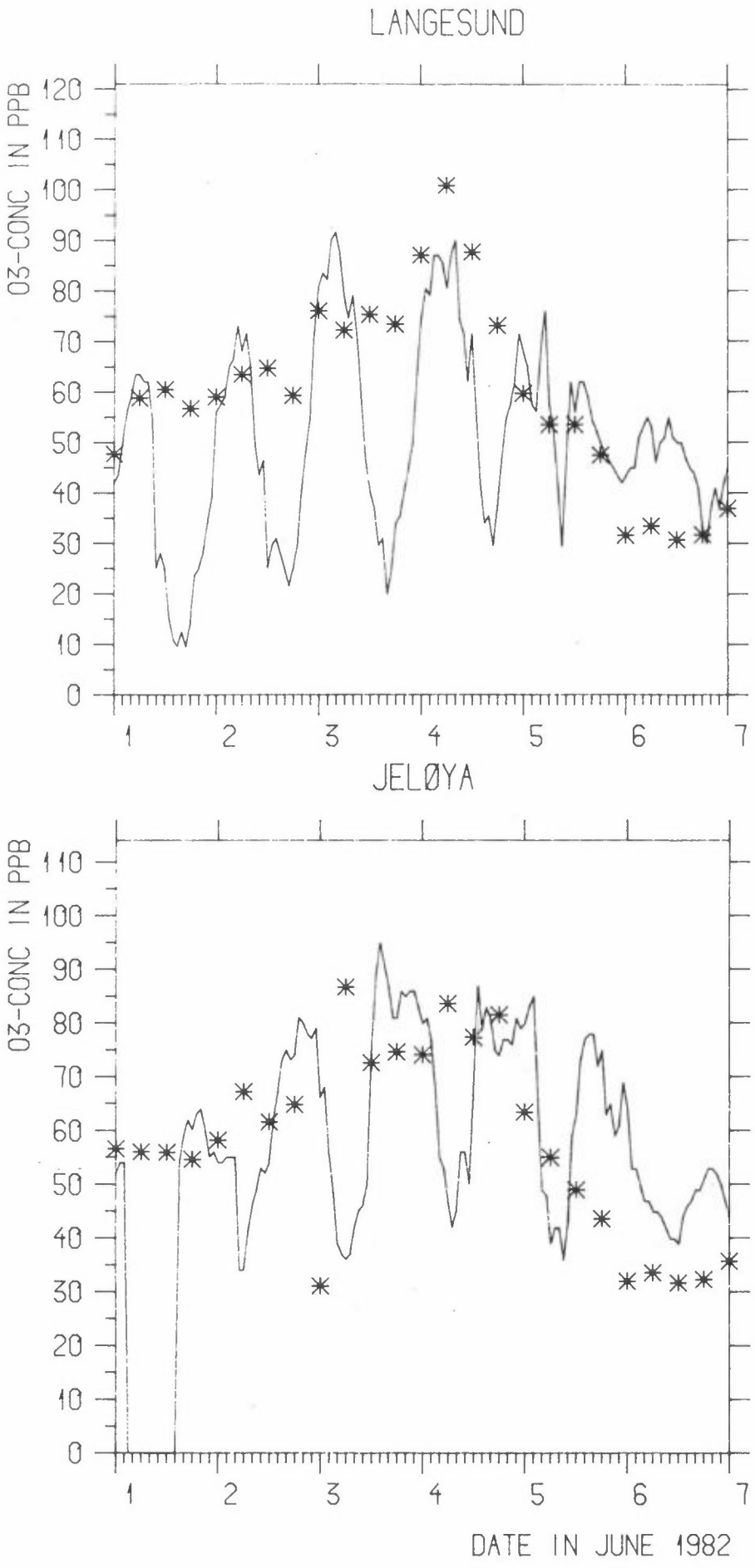
LANGESUND
O3-CONC IN PPB
0
10
20
30
40
50
60
70
80
90
100
110
120
1
2
3
4
5
6
7
JELØYA
O3-CONC IN PPB
0
10
20
30
40
50
60
70
80
90
100
110
1
2
3
4
5
6
7
DATE IN JUNE 1982

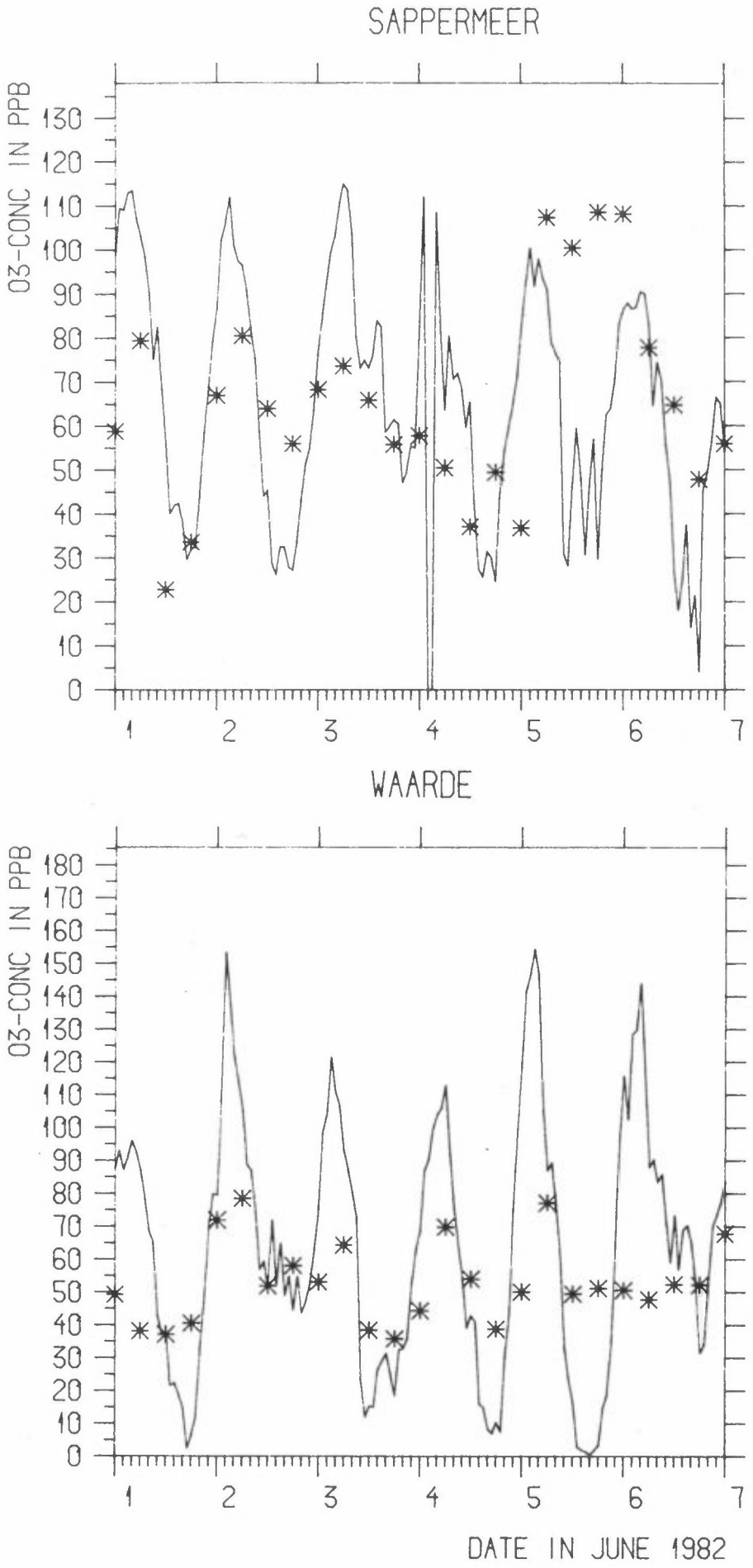
SAPPERMEER
O3-CONC IN PPB
0
10
20
30
40
50
60
70
80
90
100
110
120
130
1
2
3
4
5
6
7
WAARDE
O3-CONC IN PPB
0
10
20
30
40
50
60
70
80
90
100
110
120
130
140
150
160
170
180
1
2
3
4
5
6
7
DATE IN JUNE 1982

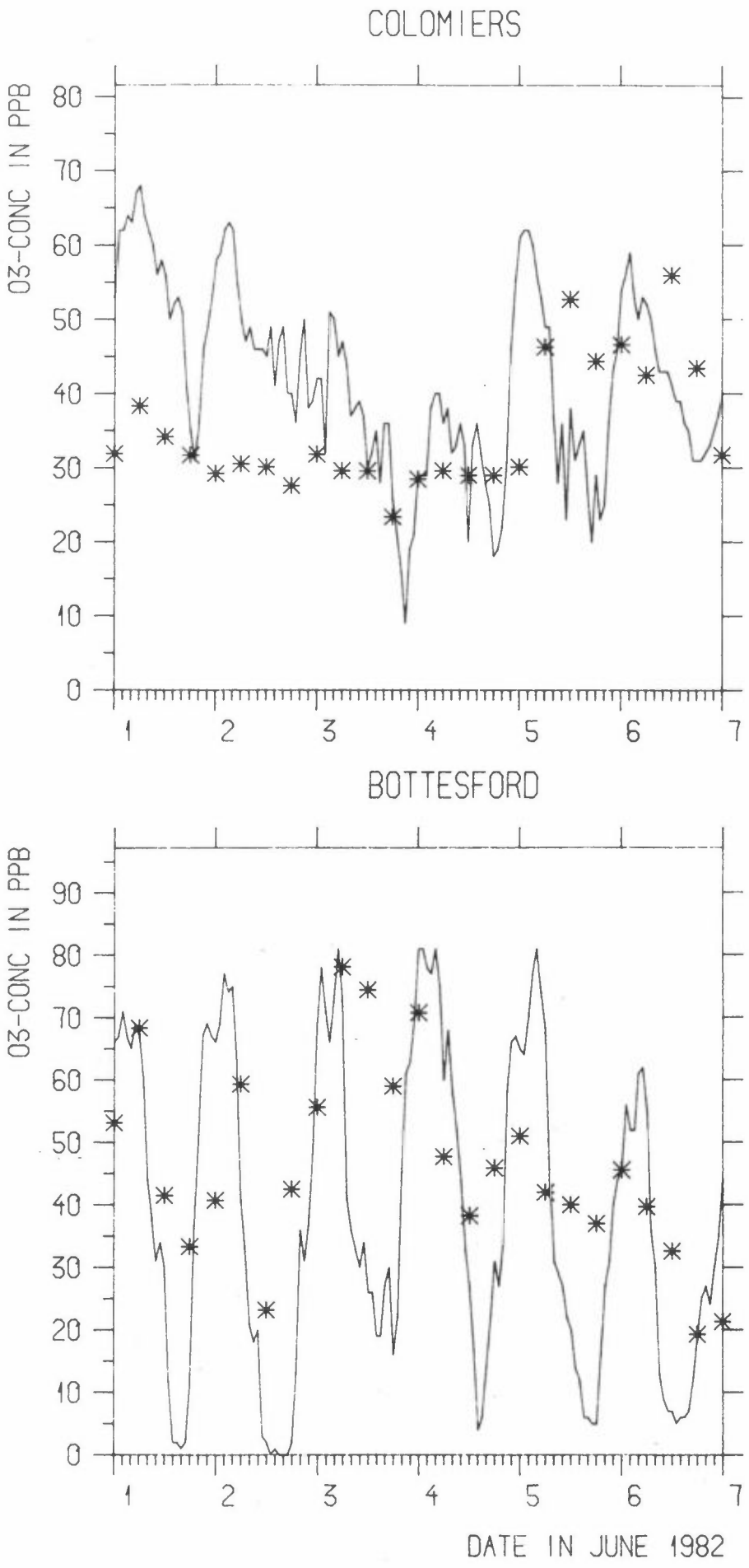
COLOMIERS
O3-CONC IN PPB
0
10
20
30
40
50
60
70
80
1
2
3
4
5
6
7
BOTTESFORD
O3-CONC IN PPB
0
10
20
30
40
50
60
70
80
90
1
2
3
4
5
6
7
DATE IN JUNE 1982

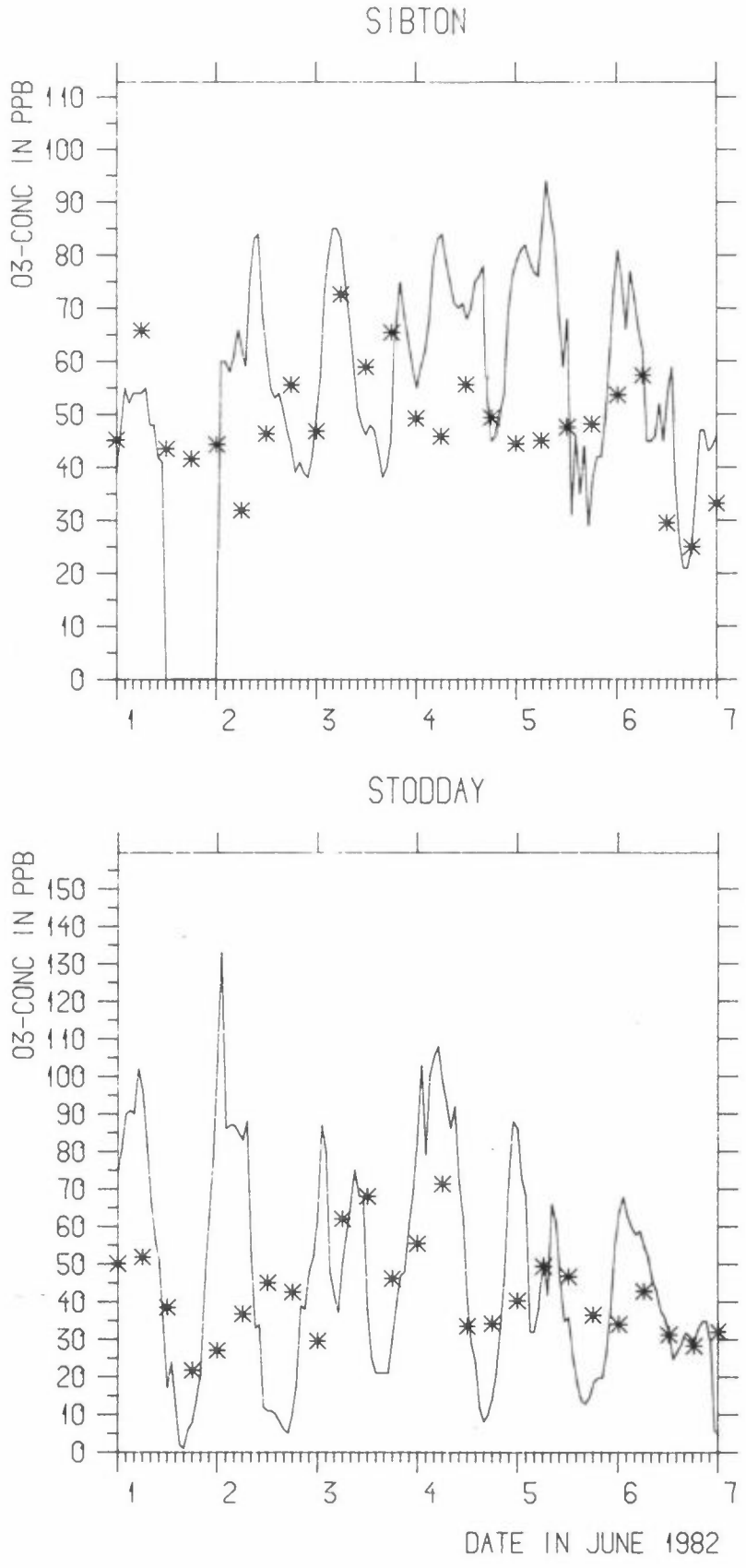

Figure 6: Hourly measured ozone concentrations vs. calculated ozone concentrations every 6 h, as a function of time starting at 1200 GMT 1 June 1982 (Day number 1) ending at 1200 GMT 7 June 1982 (Day number 7).

APPENDIX

Reproduced from Whitten et al. (1984).

The expanded Carbon-Bond Mechanism (CBM-X).

	REACTIONS		RATE CONSTANTS[b]	ACTIVAT. ENERGY (K)[c]
1	NO_2	= NO + O	vary	
2	O + O_2 + M	= O_3	2.22-5	-690.
3	O_3 + NO	= NO_2	26.6	1430.
4	O + NO_2	= NO	1.38 + 4	
5	O + NO_2 + M	= NO_3	2.32-3	-600.
6	O + NO + M	= NO_2	0.00312	-411.
7	NO_2 + O_3	= NO_3	4.74-2	2450.
8	O_3	= O1D	vary	
9	O_3	= O	4.2 - 2 x k_1	
10	O1D + M	= O	4.29 + 4	-100.
11	O1D + H_2O	= OH + OH	3.26 + 5	
12	O_3 + OH	= HO_2	100.0	940.
13	O_3 + HO_2	= OH	3.0	580.
14	NO_3 + NO	= NO_2 + NO_2	2.81 + 4	-250.
15	NO_3 + NO_2	= NO + NO_2	0.59	1230.
16	NO_3 + NO_2 + M	= N_2O_5	1776.0	-226.
17	N_2O_5 + H_2O	= HNO_3 + HNO_3	1.9-6	
18	N_2O_5 + M	= NO_3 + NO_2	3.12-6	10650.
19	NO + NO_2 + H_2O	= HNO_2 + HNO_2	1.6-11	
20	HNO_2 + HNO_2	= NO + NO_2 + H_2O	1.5-5	
21	HNO_2	= NO + OH	0.18 x k_1	
22	NO_2 + OH + M	= HNO_3	1.63-2	-560.
23	NO + OH + M	= HNO_2	9.77-3	-427.
24	HO_2 + NO	= OH + NO_2	1.23 + 4	-240.
25	NO + NO + O_2	= NO_2 + NO_2	7.28-10	-530.
26	H_2O_2	= OH + OH	1.4-3	
27	OH + H_2O_2	= HO_2	2520.0	187.
28	OH + HNO_2	= NO_2	9770.0	
29	OH + HNO_3	= NO_3	192.0	-778.
30	NO_3	= NO_2 + O	26.0 x k_1	
31	NO_3	= NO	4.6 x k_1	
32	HO_2 + HO_2	= H_2O_2	4144.0	-1150.
33	HO_2 + HO_2 + H_2O	= H_2O_2 + H_2O	0.218	-5800.
34	HO_2 + NO_2 + M	= PNA	1.63-3	-617.
35	PNA + M	= HO_2 + NO_2	5.12-6	10420.

36	$OH + CO + M$	$= HO_2$	4.0-4	
37	$FORM + HO_2$	= FROX	14.8	
38	$FORM + OH$	$= HO_2 + CO$	1.5 + 4	
39	FORM	$= HO_2 + HO_2 + CO$	vary	
40	FORM	= CO	vary	
41	FORM + O	$= OH + HO_2 + CO$	237.0	1550.
42	$FORM + NO_3$	$= HNO_3 + HO_2 + CO$	0.93	
43	FROX + NO	$= FACD + NO_2 + HO_2$	10400.0	
44	FROX	$= HO_2 + FORM$	90.0	
45	ALD2 + O	$= C_2O_3 + OH$	636.0	986.
46	ALD2 + OH	$= C_2O_3$	24000.0	-250.
47	$ALD2 + NO_3$	$= C_2O_3 + HNO_3$	3.7	
48	ALD2	$= MEO_2 + HO_2 + CO$	vary	
49	$ALD2 + HO_2$	$= MEO_2$ + FORM	5.0	
50	$C_2O_3 + NO$	$= MEO_2 + NO_2$	16500.0	-250.
51	$C_2O_3 + NO_2$	= PAN	9000.0	-250.
52	PAN	$= C_2O_3 + NO_2$	0.0222	14000.
53	$MEO_2 + NO_2 + M$	= MPNA	6.00-3	-735.
54	MPNA + M	$= MEO_2 + NO_2$	9.2-5	10400.
55	$MEO_2 + NO$	$= MEO + NO_2$	11000.0	-180.
56	MEO + NO	= MNIT	44400.0	-200.
57	MEO + NO	$= FORM + HO_2 + NO$	1920.0	
58	$MEO + NO_2$	= MEN3	22200.0	
59	$MEO + O_2$	$= FORM + HO_2$	1.88	1313.
60	MEN3 + OH	$= FORM + NO_2$	2220.0	360.
61	MNIT + OH	= FORM + NO	2370.0	340.
62	MNIT	$= MEO + NO$	$0.3 \times k_1$	
63	$MEO_2 + MEO_2$	= MEO + MEO	0 75.0	-220.
64	$MEO_2 + MEO_2$	= FORM + MEOH	328.0	-220.
65	$MEO_2 + C_2O_3$	$= MEO + MEO_2$	4400.0	
66	$C_2O_3 + C_2O_3$	$= MEO_2 + MEO_2$	3700.0	
67	$MEO_2 + O_2$	= FORM	8900.0	-1300.
68	$C_2O_3 + HO_2$	= PROX	9600.0	
69	AONE	$= MEO_2 + C_2O_3$	$0.0002 \times k_1$	
70	AONE + OH	$= ANO_2$	580.0	
71	$ANO_2 + NO$	$= NO_2 + FORM + C_2O_3$		12000.0
72	GLY	= CO + CO	$0.0052 \times k_1$	
73	GLY	= CO + FORM	$0.0016 \times k_1$	
74	GLY	$= HO_2 + HO_2 + CO + CO$		0.0007

75	GLY + OH	= HO_2 + CO + CO	15000.0	
76	MGLY	= C_2O_3 + HO_2 + CO	0.02 x k_1	
77	MGLY + OH	= MGPX	26000.0	
78	MGPX + NO	= C_2O_3 + NO_2	12000.0	
79	OH + M	= MEO_2	2.1-5	
80	PAR + OH	= RO_2	150.0	
81	PAR + OH	= RO_2R	1000.0	
82	RO_2 + NO	= NO_2 + HO_2 + ALD2 + X	12000.0	
83	RO_2R + NO	= NO_2 + ROR	12000.0	
84	RO_2R + NO	= NTR	1000.0	
85	ROR + NO_2	= NTR	22000.0	
86	ROR	= KET + HO_2	150000.0	
87	ROR	= ALD2 + D	90000.0	7000.
88	ROR	= AONE + D + X + X	240000.0	
89	X + PAR		10000.0	
90	D + PAR	= RO_2	3000.0	
91	D + PAR	= AO_2 + X + X	7000.0	
92	D + KET	= C_2O_3	10000.0	
93	AO_2 + NO	= NO + HO_2 + AONE	12000.0	
94	KET	= C_2O_3 + RO_2 + X + X		0.0003 x k_1
95	O + OLE	= MEO_2 + C_2O_3 + X	300.0	324.
96	O + OLE	= RO_2 + HO_2 + CO + X		880.
97	O + OLE	= ALD2	4740.0	324.
98	OH + OLE	= MEO_2 + ALD2 + X	42000.0	-537.
99	O_3 + OLE	= ALD2 + CRIG	0.0054	1897.
101	O_3 + OLE	= ALD2 + HOTA	0.0036	1897.
102	O_3 + OLE	= FORM + HTMA	0.0036	1897.
103	NO_3 + OLE	= PNO_2	11.4	
104	O + ETH	= MEO_2 + HO_2 + CO	1080.0	800.
105	OH + ETH	= MEO_2 + FORM	1.2E + 4	-382.
106	O_3 + ETH	= FORM + CRIG	0.001	2840.
107	O_3 + ETH	= FORM + HOTA	0.0017	2840.
108	HOTA		25.0	
109	HOTA	= CO	58.0	
110	HOTA	= HO_2 + HO_2	10.0	
111	HOTA	= FACD	7.0	
112	HTMA		200.0	
113	HTMA	= MEO_2 + CO + OH	400.0	

114	HTMA	= MEO_2 + HO_2	320.0	
115	HTMA	= HO_2 + CO + FORM + HO_2	80.0	
116	CRIG + NO	= FORM + NO_2	10000.0	
117	CRIG + NO_2	= FORM + NO_3	1000.0	
118	CRIG + H_2O	= FACD	0.006	
119	CRIG + FORM	= OZD	30.0	
120	CRIG + ALD2	= OZD	30.0	
121	MCRG + NO	= ALD2 + NO_2	10000.0	
122	MCRG + NO_2	= ALD2 + NO_3	1000.0	
123	MCRG + H_2O	= ACAC	0.006	
124	MCRG + FORM	= OZD	30.0	
125	MCRG + ALD2	= OZD	30.0	
126	PNO_2 + NO	= DNIT	1000.0	
127	PNO_2 + NO	= NTR + HO_2 + NO_2	10000.0	
128	TOL + OH	= OPEN + GLY	5500.0	
129	TOL + OH	= PHEN + HO_2	3500.0	
130	TOL + OH	= BO_2	750.0	
131	OPEN + NO	= NO_2 + HO_2 + MGLY + GLY	10000.0	
132	PHEN + NO_3	= PHO + HNO_3	14000.0	
133	BZA + OH	= BZO_2	20000.0	
134	BZO_2 + O_2	= PBZN	2500.0	
135	BZO_2 +NO	= NO_2 + PHO_2 + CO	3700.0	
136	BO_2 + NO	= NO_2 + BZA + HO_2	12000.0	
137	PBZN	= BZO_2 + O_2	0.022	14000.
138	BZA		0.004 x k_1	
139	PHO + NO_2	= NPHN	20000.0	
140	PHO_2 + NO	= NO_2 + PHO	12000.0	
141	XYL + OH	= XYLO	2000.0	
142	XYLO + NO	= NO_2 + HO_2 + TLA	12000.0	
143	TLA + OH	= TLO_2	20000.0	
144	TLO_2 + NO	= NO_2 + PHO	4000.0	
145	XYL + OH	= HO_2 + PHEN	10000.0	
146	XYL+ OH	= OPEN + MGLY	24000.0	

b All rate constants are in appropriate ppm and min units at 298K and one atmosphere of air. That is, all unimolecular and photolysis reactions (+ hν) are in units of min^{-1}, all bimolecular reactions are in units of ppm^{-1} min^{-1}, and all ter-molecular reactions are in units of ppm^{-2} min^{-1}. Powers of ten are indicated by + or - n.

c The numbers listed are Arrhenious temperature coefficients in degrees Kelvin for B in the expression $k = Aexp(-B/T)$.

NORSK INSTITUTT FOR LUFTFORSKNING (NILU)
NORWEGIAN INSTITUTE FOR AIR RESEARCH
POSTBOKS 64, N-2001 LILLESTRØM

RAPPORTTYPE	RAPPORTNR.	ISBN
OPPDRAGSRAPPORT	OR 72/87	ISBN-82-7247-870-6

DATO	ANSV. SIGN.	ANT. SIDER	PRIS
DECEMBER 1987	J. Schjoldager	52 2	kr 50,-

TITTEL
The abatement of photochemical oxidants in Europe. Calculations in the support of OECD's project "Control of major air pollutants".

PROSJEKTLEDER
Øystein Hov

NILU PROSJEKT NR.
N-8434 O-8437

FORFATTER(E)
Øystein Hov

TILGJENGELIGHET
A

OPPDRAGSGIVERS REF.

OPPDRAGSGIVER (NAVN OG ADRESSE)
NTNF, SFT

3 STIKKORD (à maks. 20 anslag)
Photochemical oxidants | Episodes | Control strategies

REFERAT (maks. 300 anslag, 7 linjer)

TITLE

ABSTRACT (max. 300 characters, 7 lines)
The Norwegian lagrangian long-range transport model with CBM-X chemistry has been applied to calculate the concentration of ozone and other photochemical oxidants at 14 measuring sites in Europe 1-7 June 1982. Reduction of VOC-emissions is calculated to reduce ozone. Reduction of NOx or NOx and VOC together is less efficient.

* Kategorier: Åpen - kan bestilles fra NILU A
Må bestilles gjennom oppdragsgiver B
Kan ikke utleveres C